Immunity, Vol. 21, 843–851, December, 2004, Copyright ©2004 by Cell Press

Enhanced Self-Renewal of Hematopoietic Stem Cells Mediated by the Polycomb Gene Product Bmi-1

Atsushi Iwama,[1,6,*] Hideyuki Oguro,[1,6] Masamitsu Negishi,[1] Yuko Kato,[1] Youhei Morita,[1] Hiroko Tsukui,[1] Hideo Ema,[1] Takehiko Kamijo,[2] Yuko Katoh-Fukui,[3] Haruhiko Koseki,[4] Maarten van Lohuizen,[5] and Hiromitsu Nakauchi[1,*]

[1]Laboratory of Stem Cell Therapy
Center for Experimental Medicine
The Institute of Medical Science
University of Tokyo
Tokyo 108-8639
Japan

[2]Department of Pediatrics
Shinshu University School of Medicine
Nagano 390-8621
Japan

[3]Department of Developmental Biology
National Institute for Basic Biology
Aichi 444-8585
Japan

[4]Laboratory for Developmental Genetics
RIKEN Research Center for Allergy and Immunology
Yokohama 230-0045
Japan

[5]Division of Molecular Genetics
The Netherlands Cancer Institute
1066 CX Amsterdam
The Netherlands

Summary

The Polycomb group *(PcG)* gene *Bmi-1* has recently been implicated in the maintenance of hematopoietic stem cells (HSC) from loss-of-function analysis. Here, we demonstrate that increased expression of *Bmi-1* promotes HSC self-renewal. Forced expression of *Bmi-1* enhanced symmetrical cell division of HSCs and mediated a higher probability of inheritance of stemness through cell division. Correspondingly, forced expression of *Bmi-1*, but not the other *PcG* genes, led to a striking ex vivo expansion of multipotential progenitors and marked augmentation of HSC repopulating capacity in vivo. Loss-of-function analyses revealed that among *PcG* genes, absence of *Bmi-1* is preferentially linked with a profound defect in HSC self-renewal. Our findings define Bmi-1 as a central player in HSC self-renewal and demonstrate that Bmi-1 is a target for therapeutic manipulation of HSCs.

Introduction

Cell-type specific gene expression patterns are stabilized by changes in chromatin structure. Cellular memory of chromatin modifications can be faithfully maintained through subsequent cell divisions by the counteractions of transcriptional activators of the trithorax group (TrxG) proteins and repressors of the PcG (Jacobs and van Lohuizen, 2002; Orland, 2003). PcG proteins form multiprotein complexes that play an important role in the maintenance of transcriptional repression of target genes. At least two distinct PcG complexes have been identified and well characterized. One complex includes Eed, EzH1, and EzH2, and the other includes Bmi-1, Mel-18, Mph1/Rae28, M33, Scmh1, and Ring1A/B. Eed-containing complexes control gene repression through recruitment of histone deacetylase followed by local chromatin deacetylation and by methylation of histone H3 Lysine 27 by EzH2. In contrast, no enzymatic activity has yet been reported with regard to Bmi-1-containing complexes. However, Bmi-1 complexes antagonize chromatin remodeling by the SWI-SNF complex (Shao et al., 1999) and are recruited to methylated histone H3 Lysine 27 via M33 chromodomain to contribute to the static maintenance of epigenetic memory (Fischle et al., 2003). These two types of complexes coordinately maintain positional memory along the anterior-posterior axis by regulating *Hox* gene expression patterns during development (Jacobs and van Lohuizen, 2002; Orland, 2003). On the other hand, these two complexes play reciprocal roles in definitive hematopoiesis: negative regulation by the Eed-containing complex and positive regulation by Bmi-1-containing complex (Lessard et al., 1999).

The Bmi-1-containing complex has been implicated in the maintenance of hematopoietic and leukemic stem cells (HSC) (Ohta et al., 2002; Park et al., 2003; Lessard and Sauvageau, 2003). *Mph1/Rae28*$^{-/-}$ fetal liver contains 20-fold fewer long-term lymphohematopoietic repopulating HSCs than wild-type (wt) (Ohta et al., 2002). More importantly, although *Bmi-1*$^{-/-}$ mice show normal development of embryonic hematopoiesis, *Bmi-1*$^{-/-}$ HSCs have a profound defect in self-renewal capacity. They cannot repopulate hematopoiesis long term, leading to progressive postnatal pancytopenia (Park et al., 2003; van der Lugt et al., 1994). Notably, the self-renewal defect is not only confined to HSC but also applicable to leukemic stem cells and neuronal stem cells (Lessard and Sauvageau, 2003; Molofsky et al., 2003). So far, the defective self-renewal of HSC has been attributed to derepression of Bmi-1 target genes $p16^{Ink4a}$ and $p19^{Arf}$, and deficiency of these genes partially reverses the self-renewal defect in *Bmi-1*$^{-/-}$ stem cells (Park et al., 2003; van der Lugt et al., 1994; Molofsky et al., 2003; Jacobs et al., 1999). More recently, Bmi-1 was reported also to be essential to the expansion of cerebellar granule cell progenitors, in which *Bmi-1* expression is reportedly regulated by the sonic hedgehog pathway (Leung et al., 2004). All of these findings have uncovered novel aspects of stem cell regulation exerted by epigenetic modifications. However, the defects in HSC in *Bmi-1*$^{-/-}$ mice has not yet been characterized in detail at the clonal level in vitro and in vivo. Furthermore, important questions remain, including the role of each component of the PcG complex in HSC and the impact of forced expression of *Bmi-1* on HSC self-renewal.

*Correspondence: aiwama@ims.u-tokyo.ac.jp (A.I.); nakauchi@ims.u-tokyo.ac.jp (H.K.)
[6]These authors contributed equally to this work.

A

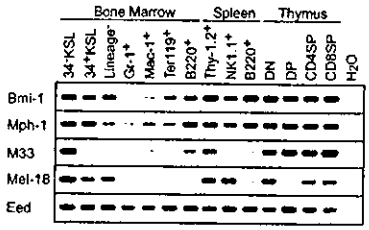

B

	E14.5 FL donor cells			Competitor Ly5.1 cells	PB chimerism 4 w	PB chimerism 12 w	
Bmi-1	+/+	$2x10^6$	(n=10)	$2x10^5$	90.2 ± 1.2	95.0 ± 1.2	
	+/–	$2x10^6$	(n=9)	$2x10^5$	86.1 ± 3.0	93.0 ± 2.4	*
	–/–	$2x10^6$	(n=10)	$2x10^5$	0.7 ± 0.5	0.4 ± 0.4	
Mel-18	+/+	$2x10^6$	(n=19)	$2x10^5$	86.1 ± 4.3	88.9 ± 2.9	*
	–/–	$2x10^6$	(n=7)	$2x10^5$	62.1 ± 5.0	64.9 ± 9.0	
M33	+/+	$2x10^6$	(n=3)	$2x10^5$	94.0 ± 2.3	98.9 ± 0.7	
	–/–	$2x10^6$	(n=2)	$2x10^5$	90.3	99.2	

* p<0.0001

Figure 1. Role of Components of the Bmi-1-Containing Complex in HSC

(A) mRNA expression of mouse *PcG* genes in hematopoietic cells. Cells analyzed are bone marrow CD34$^-$c-Kit$^+$Sca-1$^+$Lineage marker$^-$ stem cells (CD34$^-$KSL), CD34$^+$KSL progenitors, Lineage marker$^-$ cells (Lin$^-$), Gr-1$^+$ neutrophils, Mac-1$^+$ monocytes/macrophages, TER119$^+$ erythroblasts, B220$^+$ B cells, spleen Thy-1.2$^+$ T cells, NK1.1$^+$ NK cells, B220$^+$ B cells, and thymic CD4$^-$CD8$^-$ T cells (DN), CD4$^-$CD8$^+$ T cells (DP), CD4$^+$CD8$^-$ T cells (CD4SP), and CD4$^-$CD8$^+$ (CD8SP).

(B) Competitive lymphohematopoietic repopulating capacity of *PcG* gene-deficient HSCs. The indicated number of E14 fetal liver cells from *Bmi-1*$^{-/-}$, *Mel-18*$^{-/-}$, or *M33*$^{-/-}$ mice (B6-Ly5.2) and B6-Ly5.1 competitor cells were mixed and injected into lethally irradiated B6-Ly5.1 recipient mice. Percent chimerism of donor cells 4 and 12 weeks after transplantation is presented as mean ± SD.

In this study, both loss-of-function and gain-of-function analysis revealed a central role for Bmi-1, but not the other components, in the maintenance of HSC self-renewal both in vitro and in vivo and in augmentation of HSC activity ex vivo. Our findings indicate that the expression level of Bmi-1 is the critical determinant for the self-renewal capacity of HSCs.

Results

The Role of Different Components of the Bmi-1-Containing Complex in HSC

Expression analysis of *PcG* genes in human hematopoietic cells has demonstrated that *Bmi-1* is preferentially expressed in primitive cells, whereas other *PcG* genes, including *M33*, *Mel-18*, and *Mph1/Rae-28*, are not detectable in primitive cells but upregulated along with differentiation (Lessard et al., 1998). Our detailed RT-PCR analysis of mouse hematopoietic cells, however, revealed that all *PcG* genes encoding components of the Bmi-1-containing complex, including *Bmi-1*, *Mph1/Rae-28*, *M33*, and *Mel-18*, are highly expressed in CD34$^-$KSL HSCs that comprise only 0.004% of bone marrow mononuclear cells (Osawa et al., 1996), and all are down regulated during differentiation in the bone marrow (BM) (Figure 1A). In contrast, *Eed*, whose product composes another PcG complex, was ubiquitously expressed. These expression profiles support the idea of positive regulation of HSC self-renewal by the Bmi-1-containing complex (Park et al., 2003; Lessard and Sauvageau, 2003). To evaluate the role of uncharacterized PcG components (Mel-18 and M33) in the maintenance of HSCs, we performed competitive repopulation assay with ten times more fetal liver cells from *Bmi-1*$^{-/-}$, *Mel-18*$^{-/-}$, or *M33*$^{-/-}$ mice than competitor cells. As reported, *Bmi-1*$^{-/-}$ fetal liver cells did not contribute at all to long-term reconstitution (Figure 1B). The profound defect of repopulating activity was confirmed in a radioprotection assay in which *Bmi-1*$^{-/-}$ hematopoietic cells failed to ensure long-term survival of lethally irradiated mice, although they prolonged the survival of recipients over 21 days, indicating that their short-term repopulation capacity is largely preserved (Supplemental Figure S1A available online at http://www.immunity.com/cgi/content/full/21/6/843/DC1/). Mel-18 is highly related to Bmi-1 in domain structure, particularly in their N-terminal Ring finger and helix-turn-helix domains. Unexpectedly, *Mel-18*$^{-/-}$ fetal liver cells showed a very mild deficiency in repopulating capacity when compared to *Bmi-1*$^{-/-}$ fetal liver cells (Figure 1B). Moreover, *M33*$^{-/-}$ fetal liver cells exhibited normal repopulating capacity in both primary (Figure 1B) and secondary recipients (chimerism after 3 months; wt 91.6 ± 2.0 versus *M33*$^{-/-}$ 92.2 ± 3.4, n = 4). As is the case with *Bmi-1*$^{-/-}$ fetal livers, both *Mel-18*$^{-/-}$ and *M33*$^{-/-}$ fetal livers did not show any gross abnormalities, including numbers of hematopoietic cells (data not shown). To examine the *Bmi-1*$^{-/-}$ hematopoietic microenvironment, wt BM cells were transplanted into sublethally irradiated *Bmi-1*$^{-/-}$ mice. Subsequent secondary transplantation exhibited that both *Bmi-1*$^{-/-}$ BM and spleen can support long-term lymphohematopoiesis, indicating again an intrinsic defect of *Bmi-1*$^{-/-}$ HSCs (Supplemental Figure S1B).

Defective Self-Renewal and Accelerated Differentiation of *Bmi-1*$^{-/-}$ HSCs

A progressive postnatal decrease in the number of Thy1.1^{low}c-Kit$^+$Sca-1$^+$lineage marker$^-$ HSC has been observed in *Bmi-1*$^{-/-}$ mice (Park et al., 2003). We also observed approximately 10-fold fewer total CD34$^-$KSL HSCs as measured by flow cytometry in 8-week-old *Bmi-1*$^{-/-}$ mice (data not shown). To evaluate the proliferative and differentiation capacity of *Bmi-1*$^{-/-}$ HSCs in BM, we purified the CD34$^-$KSL HSC fraction, which is highly enriched for long-term repopulating HSCs (Osawa et al., 1996). *Bmi-1*$^{-/-}$ CD34$^-$KSL cells showed comparable proliferation with wt and *Bmi-1*$^{+/-}$ cells for the first week of culture, but thereafter, they proliferated poorly (Figure 2A). Single cell growth assays demonstrated that *Bmi-1*$^{-/-}$ CD34$^-$KSL cells are able to form detectable colonies at a frequency comparable to *Bmi-1*$^{+/+}$ and *Bmi-1*$^{+/-}$ CD34$^-$KSL cells but contained 3-fold fewer high-proliferative-potential colony-forming cells (HPP-CFCs). Reduction of HPP-CFCs that gave rise to colonies larger than 2 mm in diameter was even more prominent (7-fold) (Figure 2B). All HPP colonies larger than 1 mm in diameter were evaluated morphologically. Surprisingly, most of the HPP colonies generated from *Bmi-1*$^{-/-}$ CD34$^-$KSL cells consisted of only neutrophils

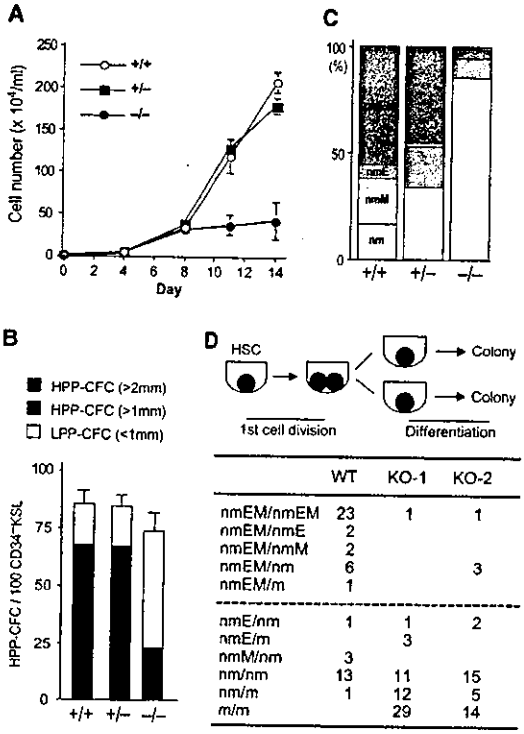

	WT	KO-1	KO-2
nmEM/nmEM	23	1	1
nmEM/nmE	2		
nmEM/nmM	2		
nmEM/nm	6		3
nmEM/m	1		
nmE/nm	1	1	2
nmE/m		3	
nmM/nm	3		
nm/nm	13	11	15
nm/m	1	12	5
m/m		29	14

Figure 2. Defective Self-Renewal and Accelerated Differentiation of *Bmi-1*$^{-/-}$ HSCs

(A) Growth of *Bmi-1*$^{-/-}$ CD34$^-$KSL HSCs in vitro. Freshly isolated CD34$^-$KSL cells were cultured in the presence of SCF, IL-3, TPO, and EPO for 14 days. The results are shown as mean ± SD of triplicate cultures.

(B) Single cell growth assay. 96 individual CD34$^-$KSL HSCs were sorted clonally into 96-well microtiter plates in the presence of SCF, IL-3, TPO, and EPO. The numbers of high- and low-proliferative-potential colony-forming cells (HPP-CFC and LPP-CFC) were retrospectively evaluated by counting colonies at day 14 (HPP-CFC and LPP-CFC: colony diameter >1 mm and <1 mm, respectively). The results are shown as mean ± SD of triplicate cultures.

(C) Frequency of each colony type. Colonies derived from HPP-CFC were recovered and morphologically examined for the composition of colony-forming cells.

(D) Paired daughter assay. When a single CD34$^-$KSL HSC underwent cell division and gave rise to two daughter cells, daughter cells were separated by micromanipulation and were further cultured to permit full differentiation along the myeloid lineage. The colonies were recovered for morphological examination.

and macrophages. *Bmi-1*$^{-/-}$ CD34$^-$KSL cells presented a 9-fold reduction in their frequency of colony-forming unit-neutrophil/macrophage/erythroblast/megakaryocyte (CFU-nmEM), which retains multilineage differentiation capacity compared with *Bmi-1*$^{+/+}$ CD34$^-$KSL cells (Figure 2C). Failure of *Bmi-1*$^{-/-}$ CD34$^-$KSL cells to inherit multilineage differentiation potential through successive cell division was obvious in a paired daughter assay (Figure 2D). In most daughter cell pairs generated from wt CD34$^-$KSL cells, at least one of the two daughter cells inherited nmEM differentiation potential, whereas *Bmi-1*$^{-/-}$ CD34$^-$KSL cells showed accelerated loss of multilineage differentiation potential, leading to the limited differentiation and inefficient expansion of their progeny. In terms of differentiation, no apparent differentiation block has been observed in *Bmi-1*$^{-/-}$ lymphocytes despite their reduced numbers (Jacobs et al., 1999). Analysis of myeloid progenitors in BM did not detect any proportional deviations of common myeloid progenitors (CMP), granulocyte/macrophage progenitors (GMP), or megakaryocyte/erythroid progenitors (MEP) either (Supplemental Figure S2), indicating that abnormal hematopoiesis observed in *Bmi-1*$^{-/-}$ mice does not accompany any specific differentiation block in myeloid lineages.

These profound defects of *Bmi-1*$^{-/-}$ HSC function evoke the possibility that absence of Bmi-1 in HSCs causes additional epigenetic abnormalities that are irreversible, and CD34$^-$KSL cells do not retain stem cell properties anymore. Retroviral transduction of *Bmi-1*$^{-/-}$ CD34$^-$KSL cells with *Bmi-1*, however, completely rescued their defects in proliferation and multilineage differentiation potential in vitro (Figures 3A and 3B) and long-term repopulating capacity in vivo (Figure 3D). These findings suggest that execution of stem cell activity is absolutely dependent on Bmi-1. Because *Mel-18*$^{-/-}$ and *M33*$^{-/-}$ mice in a C57BL/6 background die during the perinatal period or soon after birth, we could not evaluate their roles in adult BM HSCs. We next asked if HoxB4, a well-characterized HSC regulator, could rescue *Bmi-1*$^{-/-}$ phenotypes. Real-time PCR analysis demonstrated that *HoxB4* expression is not significantly affected in freshly isolated *Bmi-1*$^{-/-}$ KSL cells (relative expression in *Bmi-1*$^{-/-}$ to wt KSL cells, 0.73 ± 0.21, n = 3, p = 0.4). Interestingly, expression of *HoxB4* did not rescue *Bmi-1*$^{-/-}$ HSC defects at all (Figures 3C and 3D), indicating that HoxB4 requires functional Bmi-1 to execute its activity in HSCs.

Given the reported involvement of derepression of *p16*^{Ink4a} and *p19*^{Arf} genes in the self-renewal defect in *Bmi-1*$^{-/-}$ HSCs (Park et al., 2003; Lessard and Sauvageau, 2003), we examined their expression in hematopoietic cells. As reported, both were significantly upregulated in *Bmi-1*$^{-/-}$ Lin$^-$ cells (Supplemental Figure S3A). Overexpression of *p16* inhibits G_1-S progression, and increased *p19* causes p53-dependent growth arrest and apoptosis (Jacobs and van Lohuizen, 2002; Park et al., 2003; Lessard and Sauvageau, 2003). However, cell cycle analysis of *Bmi-1*$^{-/-}$ BM cells, including KSL primitive progenitors (Supplemental Figure S3B), did not discriminate any difference between wt and *Bmi-1*$^{-/-}$ mice. Furthermore, in single cell assays, *Bmi-1*$^{-/-}$ CD34$^-$KSL HSCs underwent the first cell division in a fashion similar to that of wt control (Supplemental Figure S3C) and showed no detectable apoptotic cell death (data not shown), although total *Bmi-1*$^{-/-}$ BM cells presented a slight but significant increase in apoptotic cell percentage (Supplemental Figure S3D). In addition, retrovirally transduced *Bcl-xL* had no impact on *Bmi-1*$^{-/-}$ HSCs in vitro (Figures 3A and 3B). These findings indicate that derepression of *p16* and *p19* genes in *Bmi-1*$^{-/-}$ HSC does not largely affect the cell cycle or survival of HSCs.

Augmentation of HSC Activity by Forced *Bmi-1* Expression

An essential role of Bmi-1 in the maintenance of HSC self-renewal capacity prompted us to determine augmentation of HSC activity by *PcG* genes. CD34$^-$KSL

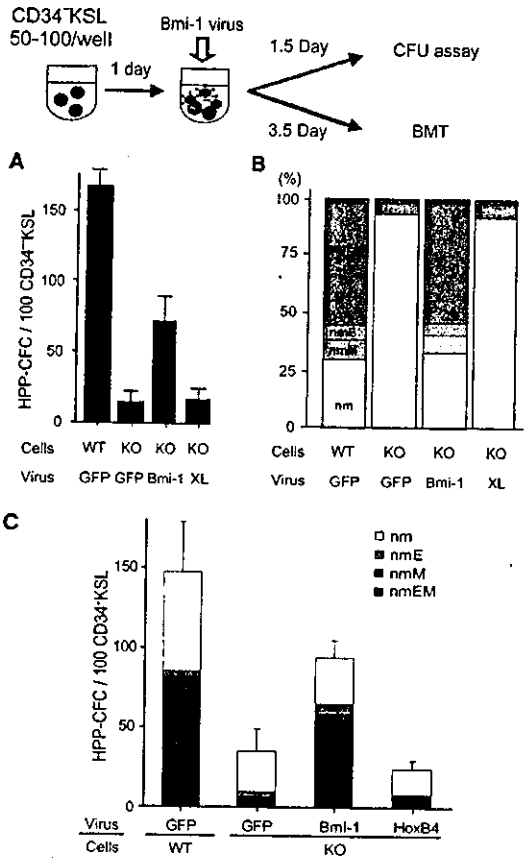

D

Virus	Donor cells Bmi-1$^{-/-}$	Competitor Ly5.1 cells	PB chimerism (%)
Bmi-1 (n=1)	80	$2x10^5$	73.0 (12 w)
Bmi-1 (n=1)	25	$2x10^5$	12.8 (12 w)
Bmi-1 (n=1)	25	$2x10^5$	13.9 (12 w)
Bmi-1 (n=4)	75	$2x10^5$	12.1±10.7 (6 w)
HoxB4 (n=4)	75	$2x10^5$	0.1±0.1 (6 w)

Figure 3. Rescue of Defective *Bmi-1*$^{-/-}$ HSC Function by Reexpression of *Bmi-1*

Wt and *Bmi-1*$^{-/-}$ CD34$^-$KSL cells were transduced with *GFP* control, *Bmi-1*, or *Bcl-xl* and plated in methylcellulose medium to allow colony formation 36 hr after the initiation of transduction. GFP$^+$ colonies larger than 1 mm in diameter, which were derived from HPP-CFCs, were counted at day 14 (A) and recovered for morphological analysis to evaluate frequency of each colony type (B). Wt and *Bmi-1*$^{-/-}$ CD34$^-$KSL cells transduced with *HoxB4* were similarly processed (C). The results are shown as mean ± SD of triplicate cultures.

(D) Indicated numbers of *Bmi-1*$^{-/-}$ CD34$^-$KSL cells were transduced with either *Bmi-1* or *HoxB4*. After 3.5 days from the initiation of transduction, cells were injected into lethally irradiated Ly5.1 recipient mice along with Ly5.1 competitor cells. Repopulation by rescued *Bmi-1*$^{-/-}$ CD34$^-$KSL cells was evaluated by monitoring donor cell chimerism in peripheral blood at the indicated time points after transplantation.

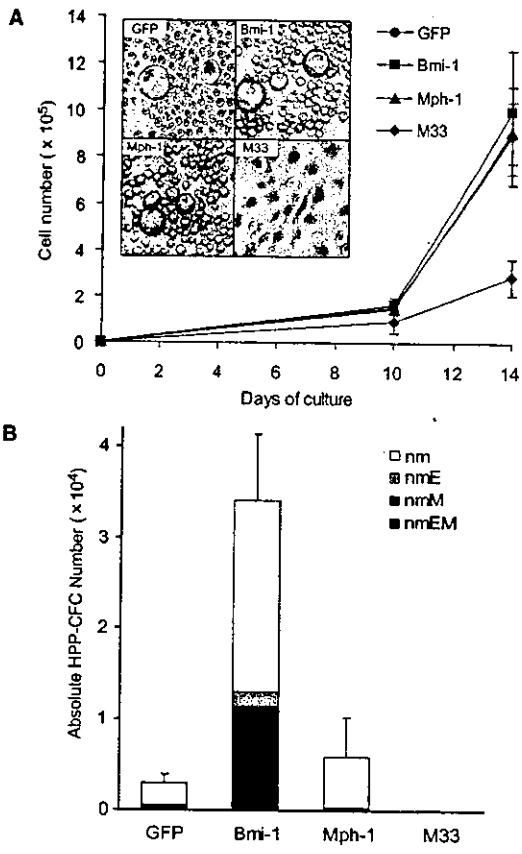

C

Fold expansion of CFU-nmEM				
Exp.1	GFP 8.6 ± 2.7	Bmi-1 81.1 ± 17.3	Mph-1 5.4 ± 4.0	M33 0 ± 0
Exp.2	GFP 1.4 ± 0.3	Bmi-1 86.1 ± 9.3	Mel-18 14.4 ± 5.1	
Exp.3	GFP 1.5 ± 0.8	Bmi-1 56.2 ± 33.4	HoxB4 37.9 ± 17.4	

Figure 4. Ex Vivo Expansion of CFU-nmEM by Forced Expression of *Bmi-1* in HSCs

(A) CD34$^-$KSL cells transduced with indicated *PcG* gene retroviruses were cultured in the presence of SCF and TPO, and their growth was monitored. Morphology of cultured cells at day 14 was observed under an inverted microscope (inset).

(B) At day 14 of culture, colony assays were performed to evaluate the content of HPP-CFC in culture. GFP$^-$ colonies derived from HPP-CFCs were examined on their colony types by morphological analysis.

(C) Net expansion of CFU-nmEM during the 14 day culture period. The results are shown as mean ± SD of triplicate cultures.

HSCs were transduced with *Bmi-1*, *Mph1/Rae28*, or *M33* and then further incubated for 13 days (14 day ex vivo culture in total). Transduction efficiencies were over 80% in all experiments (data not shown). In the presence of stem cell factor (SCF) and thrombopoietin (TPO), which support expansion of HSCs and progenitors rather than their differentiation, forced expression of *Bmi-1* as well as *Mph1/Rae28* gave no apparent growth advantage in culture compared with the *GFP* control (Figure 4A). Notably, however, *Bmi-1*-transduced, but not *Mph1/Rae28*-transduced cells, contained numerous HPP-CFCs (Figure 4B). Morphological evaluation of the

colonies revealed significant expansion of CFU-nmEM by *Bmi-1*. Given that 60% of freshly isolated CD34$^-$KSL cells can be defined as CFU-nmEM, as shown in Figure 2D, there was a net expansion of CFU-nmEM of 56- to 80-fold over 14 days in the *Bmi-1* cultures (Figure 4C). Unexpectedly, expression of *M33* induced an adverse effect on proliferation and caused accelerated differentiation into macrophages that attached to the bottom of culture dishes (Figure 4A). In contrast to *Mph-1/Rae28* and *M33*, forced expression of *Mel-18*, a polycomb gene that is highly related to *Bmi-1* in domain structure, also showed a mild but significant effect on CFU-nmEM expansion, suggestive of functional redundancy between Bmi-1 and Mel-18 (Figure 4C). The effect of *Bmi-1* is comparable to that of *HoxB4*, a well-known HSC activator (Antonchuk et al., 2002) (Figure 4C). In addition, both *Bmi-1*- and *HoxB4*-transduced cells showed higher proliferative potential and generated much larger colonies compared with the *GFP* control (data not shown).

To determine the mechanism that leads to the drastic expansion of CFU-nmEM, which retains a full range of differentiation potential, we employed a paired daughter cell assay to see if overexpression of *Bmi-1* promotes symmetric HSC division in vitro. After 24 hr of prestimulation, CD34$^-$KSL cells were transduced with a *Bmi-1* retrovirus for another 24 hr. After transduction, single cell cultures were initiated by micromanipulation. When a single cell underwent cell division, the daughter cells were separated again and were allowed to form colonies. To evaluate the commitment process of HSCs while excluding committed progenitors from this study, we selected daughter cells retaining nmEM differentiation potential by retrospective inference. Expression of *Bmi-1* was assessed by GFP expression. As expected, forced expression of *Bmi-1* significantly promoted symmetrical cell division of daughter cells (Figure 5), indicating that Bmi-1 contributes to CFU-nmEM expansion by promoting self-renewal of HSCs.

We next performed competitive repopulation assays with 10 day ex vivo cultured cells corresponding to 20 initial CD34$^-$KSL cells per recipient mouse. After 3 months, mice that received *Bmi-1*-transduced HSCs demonstrated marked enhancement of multilineage repopulation whereas repopulation mediated by *GFP*-transduced HSCs was barely detectable (Figure 6A). The repopulating potential in a cell population can be quantitated by calculating repopulation units (RU) from the donor cell chimerism and the competitor cell number (Harrison et al., 1993). *Bmi-1*-transduced HSCs manifested 35-fold higher RU compared with *GFP* controls (Figure 6B). The competitive repopulation assay was similarly performed in parallel by using *p19*$^{-/-}$ HSCs. We expected a drop in *Bmi-1*-dependent enhancement of repopulation because *p19* is one of the targets negatively regulated by Bmi-1. Actually, expression of *p19* and another Bmi-1 target gene, *p16*, was completely repressed by *Bmi-1* in cultured cells (Figure 6C). Nonetheless, expression of *Bmi-1* in *p19*$^{-/-}$ HSC again enhanced multilineage repopulation compared with *p19*$^{-/-}$ *GFP* control cells (Figure 6A). A 15-fold increase in RU was obtained with *Bmi-1*-transduced *p19*$^{-/-}$ HSCs compared to *GFP*-transduced *p19*$^{-/-}$ HSCs (Figure 6B). This data suggest that *p19* is not the main target of Bmi-1 in HSCs. Expression of other cell cycle regulator genes

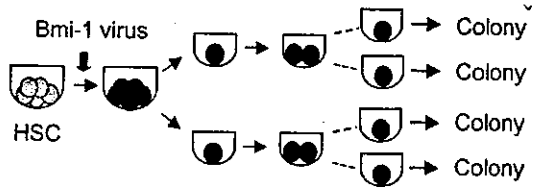

Colony pair	GFP virus	Bmi-1 virus
nmEM/nmEM	26 (53%)	40 (74%)*
nmEM/nmE	1	1
nmEM/nmM	3	6
nmEM/nm	19	7
Total	49	54

Figure 5. Forced Expression of *Bmi-1* Promotes Symmetrical Cell Division of HSCs

CD34$^-$KSL HSCs were transduced with either *GFP* or *Bmi-1* retroviruses. After 24 hr of transduction, cells were separated clonally by micromanipulation. When a single cell underwent cell division, daughter cells were separated again by micromanipulation and were further cultured to permit full differentiation along the myeloid lineage. The colonies were recovered for morphological examination. Only the pairs whose parental cells should have retained neutrophil (n), macrophage (m), erythroblast (E), and megakaryocyte (M) differentiation potential were selected. The probability of symmetrical cell division of daughter cells transduced with *Bmi-1* was significantly higher than the control ($p < 0.044$).

such as *INK4* genes (*p15*^{INK4b}, *p18*^{INK4c}, and *p19*^{INK4d}) and *Cip/Kip* genes (*p21*, *p27*, and *p57*) was not grossly affected by *Bmi-1* expression in culture (data not shown). Analysis of percent chimerism of donor cells in each hematopoietic lineage revealed that *Bmi-1*-transduced HSCs retained full differentiation capacity along myeloid and lymphoid lineages (Figure 6B). As expected from in vitro data, HSCs transduced with *M33* did not contribute to repopulation at all (Figure 6B). We further asked whether Bmi-1 could confer long-term repopulating capacity on CD34$^+$KSL progenitor cells. We transduced *Bmi-1* or *HoxB4* into CD34$^+$KSL cells and carried out both in vitro and in vivo analyses. Unexpectedly, neither *Bmi-1* nor *HoxB4* enhanced colony-forming efficiency of CD34$^+$KSL progenitor cells or conferred long-term repopulation capacity on CD34$^+$KSL progenitor cells (Supplemental Figure S4).

Discussion

Loss-of-function analyses of the *PcG* genes *Bmi-1* and *Mph1/Rae-28* have established that they are essential for the maintenance of adult BM HSCs, but not for the development of definitive HSCs (Ohta et al., 2002; Park et al., 2003; Lessard and Sauvageau, 2003). Compared with *Mph1/Rae-28*$^{-/-}$ mice, however, hematopoietic defects are more severe in *Bmi-1*$^{-/-}$ mice and are attributed to impaired HSC self-renewal (Park et al., 2003; Lessard and Sauvageau, 2003). In this study, we observed normal development of definitive hematopoiesis also in *Mel-18*$^{-/-}$ and *M33*$^{-/-}$ fetal livers. Although both

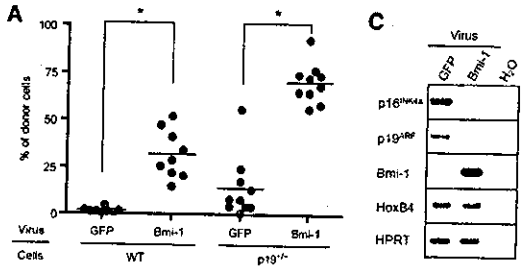

B

Mice	Virus	Percent chimerism				RU
		All WBCs	Myeloid	T Lymphoid	B Lymphoid	
WT	GFP	1.6±1.3	0.1±0.1	1.1±1.3	4.5±3.3	0.03±0.03
	Bmi-1	31.9±12.7	30.6±19.1	29.6±14.7	33.9±18.6	1.04±0.66
	M33	0	0	0	0	0
p19-/-	GFP	14.0±16.4	14.6±24.2	9.4±8.1	16.0±11.3	0.45±0.83
	Bmi-1	70.5±10.4	76.1±20.7	51.2±9.4	69.6±10.8	6.68±7.70

Figure 6. Enhancement of Repopulation Activity of HSCs by *Bmi-1* Expression

(A) $CD34^-KSL$ cells either from wt or $p19^{-/-}$ mice were transduced with indicated retroviruses and were further cultured in the presence of SCF and TPO. Competitive repopulation assays were performed by using cultured cells at day 10 corresponding to 20 initial $CD34^-KSL$ cells per recipient mouse. Percent chimerism of donor cells 12 weeks after transplantation is plotted as dots and their mean values are indicated as bars. *$p < 0.001$.

(B) Percent chimerism in each lineage and RU of each population are presented.

(C) RT-PCR analysis was performed on the wt $CD34^-KSL$ cells that were transduced with the indicated retrovirus and cultured for 14 days in the presence of SCF and TPO.

Mel-18 and *M33* genes are highly expressed in HSCs (Figure 1A), *Mel-18*$^{-/-}$ and *M33*$^{-/-}$ HSCs showed mild or no defects and retained long-term repopulating capacity (Figure 1B). Accordingly, overexpression of *PcG* genes in HSCs demonstrated that only *Bmi-1* enhances HSC function, whereas *M33* completely abolishes HSC function (Figures 4 and 6). All these findings clearly address a central role for Bmi-1 in the maintenance of HSC and suggest that the level of Bmi-1 protein is a critical determinant for the activity of the PcG complex in HSC. Bmi-1 may behave as a core component of the PcG complex in recruiting molecules essential for gene silencing or provide a docking site for DNA-binding proteins, such as Plzf on *HoxD* gene regulatory elements (Barna et al., 2002) and E2F6 that targets multimeric chromatin modifiers to E2F- and Myc-responsive genes (Trimarchi et al., 2001; Ogawa et al., 2002). On the other hand, the finding that M33 is dispensable in the maintenance of definitive HSC is surprising. Both *Bmi-1* and *M33* are involved in the maintenance of homeotic gene expression pattern through development, and strong dosage interactions between the two genes have been observed in this process (Bel et al., 1998). Our finding, however, presents a possibility that M33 does not contribute to the Bmi-1 PcG complex in HSC. M33 could be recruited to histone H3 Lysine 27 methylated by the Eed-containing complex and thereby mediate targeting of the Bmi-1-containing complex to PcG targets (Fischle et al., 2003). Thus, M33 is a key molecule for coordinated regulation of *Hox* genes by Eed- and Bmi-1-containing complexes. In contrast, the dispensable role of M33 in HSC correlated well to the reciprocal roles of the two complexes in definitive hematopoiesis (Lessard et al., 1999) and indicates that Bmi-1-containing complex has a silencing pathway of its own. The negative effect of overloaded M33 on HSCs could be due to squelching of PcG components by M33. In both loss-of-function and gain-of-function analyses, Mel-18 appeared to have a mild but significant biological function in HSCs. Given that Mel-18 shares domain structure with Bmi-1, there seems to be some functional redundancy between the two molecules in HSCs.

HSCs are maintained and expanded through self-renewal. HSC self-renewal secures its high repopulation capacity and multilineage differentiation potential through cell division. If HSCs fail to self-renew, they differentiate to lower orders of progenitors with limited proliferative and differentiation potential. Paired daughter cell assays that monitor the behavior of HSCs in vitro (Suda et al., 1984; Takano et al., 2004) demonstrated that Bmi-1 is essential for $CD34^-KSL$ cells to inherit multilineage differentiation potential through successive cell divisions (Figure 2D). Notably, overexpression of *Bmi-1* in $CD34^-KSL$ cells promoted their symmetrical cell division, indicating a higher probability of inheritance of stemness mediated by *Bmi-1* (Figure 5). This is evidence of successful genetic manipulation of HSC self-renewal in vitro. These clonal observations together with functional rescue of *Bmi-1*$^{-/-}$ HSC both in vitro and in vivo strongly support an essential role of Bmi-1 in HSC self-renewal.

The central role for Bmi-1 in HSC self-renewal was also demonstrated by overexpression experiments of *PcG* genes in HSC. The *Bmi-1*-mediated growth advantage was largely restricted to the primitive hematopoietic cells. During ex vivo culture, total cell numbers were almost comparable to the control while a net 56- to 80-fold CFU-nmEM expansion and 15- to 35-fold higher repopulation activity were obtained in the *Bmi-1* cultures (Figures 4 and 6). In agreement with these data, symmetrical cell division of HSC was promoted in the *Bmi-1* cultures (Figure 5), suggesting enhanced probability of HSC self-renewal and progenitor expansion mediated by *Bmi-1* overexpression. Importantly, transduction of *Bmi-1* into $CD34^+KSL$ progenitor cells did not enhance their colony-forming efficiency or in vivo repopulating capacity at all (Supplemental Figure S4). These findings suggest that Bmi-1 preferentially promotes HSC self-renewal and MPP expansion but does not confer growth advantage or long-term repopulation capacity on $CD34^+KSL$ progenitor cells with limited differentiation potential. Although *Bmi-1*-transduced HSC established higher repopulation in vivo, chimerism of *Bmi-1*-transduced HSC progenies reached its plateau between 2 and 3 months and never showed continuous growth advantages in vivo. This could be due to silencing of retroviral *Bmi-1* expression in vivo as suggested by a significant decrease in GFP intensity detected by flow cytometric analysis (data not shown). Actually, real-time PCR analyses demonstrated that the relative expression of *Bmi-1* in transduced cells to *GFP* control cells was 5.8 ± 1.3-fold in purified KSL cells from 14 day ex vivo culture and 1.3 ± 0.1-fold in KSL cells recovered from reconstituted recipients 6 months after transplantation. Thus, marked enhancement of HSC repopulating capacity might be obtained by enhanced HSC recovery after

ex vivo culture. Alternatively, increased expression of *Bmi-1* may not confer a growth advantage in steady-state hematopoiesis once HSC becomes quiescent in the niche. The comparable effect of *Bmi-1* to that of *HoxB4*, a well-known HSC activator (Antonchuk et al., 2002), is noteworthy. Recent findings indicated that genetic manipulation of *HoxB4* can support generation of long-term repopulating HSCs from ES cells (Kyba et al., 2002), and ex vivo expansion of HSCs can be obtained by direct targeting of HoxB4 protein into HSCs (Amsellem et al., 2003; Krosl et al., 2003). Similar to HoxB4, Bmi-1 could be a novel target for therapeutic manipulation of HSCs. Although PcG proteins regulate expression of homeotic genes including *HoxB4* during development (Takihara et al., 1997), deregulation of *Hox* genes in definitive hematopoietic cells has not yet been identified in mice deficient for *PcG* genes (Ohta et al., 2002; Park et al., 2003; Lessard and Sauvageau, 2003). In this study, *HoxB4* expression was not altered in *Bmi-1*$^{-/-}$ KSL cells or *Bmi-1*-overexpressing hematopoietic cells (Figure 6C). Moreover, forced expression of *HoxB4* failed to rescue defective *Bmi-1*$^{-/-}$ HSC function (Figures 3C and 3D). These findings are quite interesting and suggest that HoxB4 requires functional Bmi-1 to execute its function as a HSC activator. In this regard, *Bmi-1* could be epistatic to *HoxB4* or these two molecules may have some functional crosstalk in the regulation of HSC self-renewal. Actually, the enhancement of HSC activity by two genes is highly similar in many aspects. It will be intriguing to ask how these two molecules work as HSC activators.

The mechanism whereby Bmi-1 maintains HSC remains to be defined. Although derepression of the Bmi-1 target genes *p16* and *p19* has been attributed to defective HSC self-renewal, the cell cycle status of CD34$^-$KSL HSCs was not grossly altered in *Bmi-1*$^{-/-}$ mice (Supplemental Figure S3). In addition, apoptosis was not increased during observation of clonal HSC cultures, either. Therefore, a detailed analysis of *Bmi-1*$^{-/-}$*p16*$^{-/-}$ *p19*$^{-/-}$ HSCs will be necessary to define their roles in HSC. Nonetheless, *p19*$^{-/-}$ HSCs showed higher repopulating capacity than wt control (Figures 6A and 6B), and enhanced HSC repopulating capacity mediated by *Bmi-1* was correlated with repressed *p16* and p19 expression in ex vivo cultured HSCs (Figure 6C). One attractive hypothesis is that derepression of *p16* and *p19* genes causes early senescence of primitive hematopoietic cells as reported in *Bmi-1*$^{-/-}$ mouse embryonic fibroblasts (Jacobs et al., 1999). In the case of multipotent hematopoietic cells, senescence could mean accelerated differentiation and early cell cycle exit as observed in *Bmi-1*$^{-/-}$ mice. In BM, HSCs reside in a niche in close contact with supporting cells like osteoblasts (Zhang et al., 2003; Calvi et al., 2003), in which most of the HSCs stay in the G_0 stage. The quiescence of HSCs has a critical biological importance in preventing premature HSC exhaustion (Cheng et al., 2000). Taken together, HSC stemness might be maintained by a fine regulation of the cell cycle machinery.

Additional mechanisms regulating self-renewal could be responsible for preventing differentiation (Wang and Lin, 2004). We found that forced expression of *Bmi-1* inhibits differentiation of an immature hematopoietic cell line (M.N., unpublished data). It is well recognized that HSCs express most myeloid genes at a low level (Miyamoto et al., 2002). Bmi-1 in HSC might be involved in repressing differentiation-related gene expression below the level of biological significance. In this regard, the role of Bmi-1 in the function of HSC derived from C/EBPα-deficient mice is of interest. C/EBPα is a transcription factor that is required for myeloid differentiation. Of note is that C/EBPα$^{-/-}$ HSCs demonstrate increased *Bmi-1* expression and enhanced repopulation capacity and self-renewal (P. Zhang, et al., 2004 [this issue of *Immunity*]). A 3.5-fold increase in *Bmi-1* transcript level in C/EBPα$^{-/-}$ KSL cells is comparable to a 5.8-fold increase in our transduced KSL cells and thus could be sufficient to enhance HSC self-renewal capacity. Therefore, C/EBPα-deficient mice represent the first mouse model of *Bmi-1* overexpression in HSCs that recapitulates our findings described here. The increase in Bmi-1 expression may mediate many, if not all, of the phenotypic changes in C/EBPα$^{-/-}$ HSCs and may also mediate some of the block in myeloid differentiation observed in C/EBPα$^{-/-}$ mice. Further analysis of the underlying mechanisms in *Bmi-1*$^{-/-}$ cells will be needed to unveil the relative contributions of Bmi-1 to self-renewal and/or differentiation. Finally, however, because disruption of C/EBPα has been described in a number of humans with acute myeloid leukemia, it will also be of interest to investigate whether *Bmi-1* is upregulated in the leukemic blasts, and whether such upregulation contributes to the self-renewal function of leukemic stem cells, which is defective in experimental models of leukemia in cells lacking *Bmi-1* (Lessard and Sauvageau, 2003).

Experimental Procedures

Mice

Bmi-1$^{-/-}$ mice (van der Lugt et al., 1994), *Mel-18*$^{-/-}$ mice (Akasaka et al., 1996), *M33*$^{-/-}$ mice (Katoh-Fukui et al., 1998), and *p19*$^{-/-}$ mice (Kamijo et al., 1997) that had been backcrossed at least eight times onto a C57BL/6 (B6-Ly5.2) background were used in this study. C57BL/6 (B6-Ly5.2) mice were purchased from Charles River Japan, Inc. Mice congenic for the Ly5 locus (B6 Ly5.1) were bred and maintained at the Animal Research Center of the Institute of Medical Science, University of Tokyo.

Purification of Mouse Hematopoietic Stem Cells

Mouse hematopoietic stem cells (CD34$^-$KSL cells) were purified from bone marrow cells of 2-month-old mice. In brief, low-density cells were isolated on Lymphoprep (1.086 g/ml; Nycomed, Oslo, Norway). The cells were stained with an antibody cocktail consisting of biotinylated anti-Gr-1, Mac-1, B220, CD4, CD8, and Ter-119 mAbs (PharMingen, San Diego, CA). Lineage-positive cells were depleted with streptavidin-magnetic beads (M-280; Dynal Biotech, Oslo, Norway). The cells were further stained with fluorescein isothiocyanate (FITC)-conjugated anti-CD34, phycoerythrin (PE)-conjugated anti-Sca-1, and allophycocyanin (APC)-conjugated anti-c-Kit antibodies (PharMingen). Biotinylated antibodies were detected with streptavidin-Texas Red (Molecular Probes, Eugene, OR). Four-color analysis and sorting were performed on a FACS Vantage (Becton Dickinson, San Jose, CA).

Transduction of CD34$^-$KSL Cells

The murine *Bmi-1* and *Mph-1* cDNAs were FLAG-tagged at their amino terminus. The retroviral vector GCDNsam (pGCDNsam), with an LTR derived from MSCV, has intact splice donor and splice acceptor sequences for generation of subgenomic mRNA (Kaneko et al., 2001). Murine *Bmi-1*, *Mph-1*, *M33*, *Mel-18*, *Bcl-xL*, and human *HoxB4* cDNAs were subcloned into a site upstream of an *IRES-*

EGFP construct in pGCDNsam. To produce recombinant retrovirus, plasmid DNA was transfected into 293gp cells (293 cells containing the *gag* and *pol* genes but lacking an envelope gene) along with a VSV-G expression plasmid by $CaPO_4$ coprecipitation. Supernatants from transfected cells were concentrated by centrifugation at 6000 × g for 16 hr and then resuspended in α-MEM supplemented with 1% fetal calf serum (FCS) (1/200 of the initial volume of supernatant). Virus titers were determined by infection of Jurkat cells (a human T cell line). $CD34^-KSL$ cells were deposited into recombinant fibronectin fragment (Takara Shuzo, Otsu, Japan)-coated 96-well microtiter plates at 50–150 cells per well, and were incubated in α-MEM supplemented with 1% FCS, 100 ng/ml mouse stem cell factor (SCF), and 100 ng/ml human thrombopoietin (TPO) (Peprotech, Rocky Hill, NJ) for 24 hr. Then cells were transduced with a retrovirus vector at a multiplicity of infection (MOI) of 600 in the presence of protamine sulfate (5 μg/ml; Sigma, St. Louis, MO) for 24 hr. After transduction, cells were further incubated in S-Clone SF-O3 (Sanko Junyaku, Tokyo, Japan) supplemented with 1% FCS, 100 ng/ml SCF, and 100 ng/ml TPO and subjected to in vitro colony assay or competitive repopulation assay at the indicated time point. In all experiments, transduction efficiency was over 80% as judged from the GFP expression observed under a fluorescent inverted microscope.

Colony Assay

$CD34^-KSL$ cells transduced with indicated retroviruses were plated in methylcellulose medium (Stem Cell Technologies, Vancouver, BC) supplemented with 20 ng/ml mouse SCF, 20 ng/ml mouse IL-3 (Peprotech), 50 ng/ml human TPO, and 2 units/ml human erythropoietin (EPO) (Peprotech). The culture dishes were incubated at 37°C in a 5% CO_2 atmosphere. GFP^+ colony numbers were counted at day 14. Colonies derived from HPP-CFCs (colony diameter >1 mm) were recovered, cytospun onto glass slides, then subjected to May-Grüenwald Giemsa staining for morphological examination.

Paired Daughter Cell Assay

$CD34^-KSL$ cells were clonally deposited into 96-well microtiter plates in S-Clone SF-O3 supplemented with 0.1% BSA, 100 ng/ml SCF, and 100 ng/ml TPO. When a single cell underwent cell division and gave rise to two daughter cells, the daughter cells were separated into different wells by micromanipulation techniques as previously described (Suda et al., 1984; Takano et al., 2004). Individual paired daughter cells were further incubated in S-Clone SF-O3 supplemented with 10% FCS, 20 ng/ml SCF, 20 ng/ml IL-3, 50 ng/ml TPO, and 2 units/ml EPO. The colonies generated from each daughter cell were recovered for morphological examination. To evaluate the effect of Bmi-1 on HSC fate, $CD34^-KSL$ cells were transduced with a *Bmi-1* retrovirus as described above. After 24 hr transduction, cells were separated clonally by micromanipulation into 96-well microtiter plates. When a single cell underwent cell division, daughter cells were separated again by micromanipulation and were processed as described above.

Competitive Repopulation Assay

Competitive repopulation assay was performed by using the Ly5 congenic mouse system. In brief, hematopoietic cells from B6-ly5.2 mice were mixed with bone marrow competitor cells (B6-Ly5.1) and were transplanted into B6-ly5.1 mice irradiated at a dose of 9.5 Gy. In the case of Ly5.1 hematopoietic cells, cells were mixed with bone marrow competitor cells (B6-Ly5.2) and were transplanted into B6-Ly5.2 mice. 4 and 12 weeks after transplantation, peripheral blood cells of the recipients were stained with PE-conjugated anti-Ly5.1 (A20) or biotinylated anti-Ly5.2 (104) (PharMingen). The cells were simultaneously stained with PE-Cy7-conjugated anti-B220 antibody and a mixture of APC-conjugated anti-Mac-1 and anti-Gr-1 antibodies or a mixture of APC-conjugated anti-CD4 and anti-CD8 antibodies (PharMingen). The biotinylated antibody was detected with streptavidin-Texas Red. Cells were analyzed on a FACS Vantage. Percentage chimerism was calculated as (percent donor cells) × 100/(percentage donor cells + percent recipient cells). When percent chimerism was above 1.0 with myeloid, B and T lymphoid lineages, recipient mice were considered to be multilineage reconstituted (positive mice). Repopulation unit (RU) was calculated with Harrison's method (Harrison et al., 1993) as follows: RU = (percent donor cells) × (number of competitor cells) × 10^{-5}/100 − (percent donor cells). By definition each RU represents the repopulating activity of 1 × 10^5 BM cells. In this study, the number of BM competitors was fixed as 2 × 10^5 cells. T/C ratio defined above was applied to Harrison's formula as follows: RU = T/C ratio × 2.

Semiquantitative RT-PCR and Real-Time PCR

Semiquantitative RT-PCR was carried out by using normalized cDNA by the quantitative PCR with TaqMan rodent GAPDH control reagent (Perkin-Elmer Applied Biosystem, Foster City, CA) as described before (Osawa et al., 2002). PCR products were separated on agarose gels and visualized by ethidium bromide staining. Real-time PCR was done with SYBR Green PCR master mix (Perkin-Elmer Applied Biosystem) according to the manufacturer's instruction. Primer sequences and amplification conditions are available from the authors on request.

Acknowledgments

We thank Drs. T. Higashinakagawa (Waseda University, Japan), K. Humphries (Terry Fox Lab., Canada), and Dr. C.J. Sherr for providing murine *M33* cDNA, human *HoxB4* cDNA, and *p19*$^{-/-}$ mice, respectively; Dr. M. Kaneta for excellent technical assistance; and Dr. K. Etoh for critically reading the manuscript. This work was supported in part by grants from the Ministry of Education, Culture, Sport, Science, and Technology, Japan.

Received: June 17, 2004
Revised: September 30, 2004
Accepted: November 5, 2004
Published: December 14, 2004

References

Akasaka, T., Kanno, M., Balling, R., Mieza, M.A., Taniguchi, M., and Koseki, H. (1996). A role for mel-18, a Polycomb group-related vertebrate gene, during the anteroposterior specification of the axial skeleton. Development *122*, 1513–1522.

Amsellem, S., Pflumio, F., Bardinet, D., Izac, B., Charneau, P., Romeo, P.H., Dubart-Kupperschmitt, A., and Fichelson, S. (2003). Ex vivo expansion of human hematopoietic stem cells by direct delivery of the HoxB4 homeoprotein. Nat. Med. *9*, 1423–1427.

Antonchuk, J., Sauvageau, G., and Humphries, R.K. (2002). HOXB4-induced expansion of adult hematopoietic stem cells ex vivo. Cell *109*, 39–45.

Barna, M., Merghoub, T., Costoya, J.A., Ruggero, D., Branford, M., Bergia, A., Samori, B., and Pandolfi, P.P. (2002). Plzf mediates transcriptional repression of HoxD gene expression through chromatin remodeling. Dev. Cell *3*, 499–510.

Bel, S., Core, N., Djabali, M., Kieboom, K., van der Lugt, N., Alkema, M.J., and van Lohuizen, M. (1998). Genetic interactions and dosage effects of polycomb group genes in mice. Development *125*, 3543–3551.

Calvi, L.M., Adams, G.B., Weibrecht, K.W., Weber, J.M., Olson, D.P., Knight, M.C., Martin, R.P., Schipani, E., Divieti, P., Bringhurst, F.R., et al. (2003). Osteoblastic cells regulate the haematopoietic stem cell niche. Nature *425*, 841–846.

Cheng, T., Rodrigues, N., Shen, H., Yang, Y.G., Dombkowski, D., Sykes, M., and Scadden, D.T. (2000). Hematopoietic stem cell quiescence maintained by p21$^{cip1/waf1}$. Science *287*, 1804–1808.

Fischle, W., Wang, Y., Jacobs, S.A., Kim, Y., Allis, C.D., and Khorasanizadeh, S. (2003). Molecular basis for the discrimination of repressive methyl-lysine marks in histone H3 by polycomb and HP1 chromodomains. Genes Dev. *17*, 1870–1881.

Harrison, D.D., Jordan, C.T., Zhong, R.K., and Astle, C.M. (1993). Primitive hematopoietic stem cells: direct assay of most productive populations by competitive repopulation with simple binomial, correlation and covariance calculations. Exp. Hematol. *21*, 206–219.

Jacobs, J.J.L., and van Lohuizen, M. (2002). Polycomb repression:

from cellular memory to cellular proliferation and cancer. Biochim. Biophys. Acta *1602*, 151–161.

Jacobs, J.J.L., Kieboom, K., Marino, S., DePinho, R.A., and van Lohuizen, M. (1999). The oncogene and Polycomb-group gene bmi1 regulates proliferation and senescence through the ink4a locus. Nature *397*, 164–168.

Kamijo, T., Zindy, F., Roussel, M.F., Quelle, D.E., Downing, J.R., Ashmun, R.A., Grosveld, G., and Sherr, C.J. (1997). Tumor suppression at the mouse INK4a locus mediated by the alternative reading frame product p19ARF. Cell *91*, 649–659.

Kaneko, S., Onodera, M., Fujiki, Y., Nagasawa, T., and Nakauchi, H. (2001). Simplified retroviral vector gcsap with murine stem cell virus long terminal repeat allows high and continued expression of enhanced green fluorescent protein by human hematopoietic progenitors engrafted in nonobese diabetic/severe combined immunodeficient mice. Hum. Gene Ther. *12*, 35–44.

Katoh-Fukui, Y., Tsuchiya, R., Shiroishi, T., Nakahara, Y., Hashimoto, N., Noguchi, K., and Higashinakagawa, T. (1998). Male-to-female sex reversal in M33 mutant mice. Nature *393*, 688–693.

Krosl, J., Austin, P., Beslu, N., Kroon, E., Humphries, R.K., and Sauvageau, G. (2003). In vitro expansion of hematopoietic stem cells by recombinant TAT-HOXB4 protein. Nat. Med. *9*, 1428–1432.

Kyba, M., Perlingeiro, R.C.R., and Daley, G.Q. (2002). HoxB4 confers definitive lymphoid-myeloid engraftment potential on embryonic stem cell and yolk sac hematopoietic progenitors. Cell *109*, 29–37.

Lessard, J., and Sauvageau, G. (2003). Bmi-1 determines proliferative capacity of normal and leukemic stem cells. Nature *423*, 255–260.

Lessard, J., Baban, S., and Sauvageau, G. (1998). Stage-specific expression of polycomb group genes in human bone marrow cells. Blood *91*, 1216–1224.

Lessard, J., Schumacher, A., Thorsteinsdottir, U., van Lohuizen, M., Magnuson, T., and Sauvageau, G. (1999). Functional antagonism of the Polycomb-Group genes eed and Bmi1 in hematopoietic cell proliferation. Genes Dev. *13*, 2691–2703.

Leung, C., Lingbeek, M., Shakhova, O., Liu, J., Tanger, E., Saremaslani, P., van Lohuizen, M., and Marino, S. (2004). Bmi-1 is essential for cerebellar development and is overexpressed in human medulloblastomas. Nature *428*, 337–341.

Miyamoto, T., Iwasaki, H., Reizis, B., Ye, M., Graf, T., Weissman, I.L., and Akashi, K. (2002). Myeloid or lymphoid promiscuity as a critical step in hematopoietic lineage commitment. Dev. Cell *3*, 137–147.

Molofsky, A.V., Pardal, R., Iwashita, T., Park, I.K., Clarke, M.F., and Morrison, S.J. (2003). Bmi-1 dependence distinguishes neural stem cell self-renewal from progenitor proliferation. Nature *425*, 962–967.

Ogawa, H., Ishiguro, K., Gaubatz, S., Livingston, D.M., and Nakatani, Y.A. (2002). Complex with chromatin modifiers that occupies E2F- and Myc-responsive genes in G_0 cells. Science *296*, 1132–1136.

Ohta, H., Sawada, A., Kim, J.Y., Tokimasa, S., Nishiguchi, S., Humphries, R.K., Hara, J., and Takihara, Y. (2002). Polycomb group gene rae28 is required for sustaining activity of hematopoietic stem cells. J. Exp. Med. *195*, 759–770.

Orland, V. (2003). Polycomb, epigenomes, and control of cell identity. Cell *112*, 599–606.

Osawa, M., Hanada, K.I., Hamada, H., and Nakauchi, H. (1996). Long-term lymphohematopoietic reconstitution by a single CD34-low/negative hematopoietic stem cells. Science *273*, 242–245.

Osawa, M., Yamaguchi, T., Nakamura, Y., Kaneko, S., Onodera, M., Sawada, K.I., Nakauchi, H., and Iwama, A. (2002). Erythroid expansion mediated by Gfi-1B zinc finger protein: its implication in normal hematopoiesis. Blood *100*, 2769–2777.

Park, I.K., Qian, D., Kiel, M., Becker, M.W., Pihalja, M., Weissman, I.L., Morrison, S.J., and Clarke, M.F. (2003). Bmi-1 is required for maintenance of adult self-renewing haematopoietic stem cells. Nature *423*, 302–305.

Shao, Z., Raible, F., Mollaaghababa, R., Guyon, J.R., Wu, C.T., Bender, W., and Kingston, R.E. (1999). Stabilization of chromatin structure by PRC1, a polycomb complex. Cell *98*, 37–46.

Suda, T., Suda, J., and Ogawa, M. (1984). Disparate differentiation in mouse hematopoietic colonies derived paired progenitors. Proc. Natl. Acad. Sci. USA *81*, 2520–2524.

Takano, H., Ema, H., Sudo, K., and Nakauchi, H. (2004). Asymmetric division and lineage commitment at the level of hematopoietic stem cells: inference from differentiation in daughter cell and granddaughter cell pairs. J. Exp. Med. *199*, 295–302.

Takihara, Y., Tomotsune, D., Shirai, M., Katoh-Fukui, Y., Nishi, K., Motaleb, M.A., Nomura, M., Tsuchiya, R., Fujita, Y., Shibata, Y., et al. (1997). Targeted disruption of the mouse homologue of the Drosophila polyhomeotic gene leads to altered anteroposterior patterning and neural crest defects. Development *124*, 3673–3682.

Trimarchi, J.M., Fairchild, B., Wen, J., and Lees, J.A. (2001). The E2F6 transcription factor is a component of the mammalian Bmi1-containing polycomb complex. Proc. Natl. Acad. Sci. USA *98*, 1519–1524.

van der Lugt, N.M., Domen, J., Linders, K., van Roon, M., Robanus-Maandag, E., te Riele, H., van der Valk, M., Deschamps, J., Sofroniew, M., and van Lohuizen, M. (1994). Posterior transformation, neurological abnormalities, and severe hematopoietic defects in mice with a targeted deletion of the bmi-1 proto-oncogene. Genes Dev. *8*, 757–769.

Wang, Z., and Lin, H. (2004). Nanos maintains germline stem cell self-renewal by preventing differentiation. Science *303*, 2016–2019.

Zhang, J., Niu, C., Ye, L., Huang, H., He, X., Tong, W.-G., Ross, J., Haug, J., Johnson, T., Feng, J.Q., et al. (2003). Identification of the haematopoietic stem cell niche and control of the niche size. Nature *425*, 836–841.

Zhang, P., Iwasaki-Arai, J., Iwasaki, H., Fenyus, M.L., Dayaram, T., Owens, B.M., Shigematsu, H., Levantini, E., Huettner, C.S., Lekstrom-Himes, J.A., et al. (2004). Enhancement of hematopoietic stem cell repopulating capacity and self-renewal in the absence of the transcription factor C/EBPα. Immunity *21*, this issue, 853–863.

Immunity, Vol. 20, 1–4, January, 2004, Copyright ©2004 by Cell Press

"Homing to Niche," a New Criterion for Hematopoietic Stem Cells?

By combining cell surface staining with fluorochrome-conjugated monoclonal antibodies and Hoechst 33342 dye supravital staining, Matsuzaki et al. have succeeded in enriching hematopoietic stem cells (HSCs) essentially to homogeneity. When single-cell transplantation analysis was performed using the isolated cells, over 95% of the recipient mice showed long-term multilineage engraftment. The work demonstrates unexpectedly high marrow seeding efficiency of HSCs and proposes high marrow homing capacity as a new criterion for HSCs.

Stem cells are generally defined as cells capable of both self-renewal and multilineage differentiation. During development and regeneration of a given tissue, such cells give rise to non-self-renewing progenitors with restricted differentiation potential, and finally to functionally mature cells, while maintaining primitive stem cells. Because of these unique properties, stem cells offer the novel and exciting possibility of organ reconstitution in place of transplanted or artificial organs in the treatment of organ failure. Among different stem cells, hematopoietic stem cells (HSCs) are the best studied.

Purification of HSCs has progressed significantly over the last two decades, strongly assisted by well-established assay techniques. Technological advances in flow cytometry and electronic cell sorting have also aided in stem cell purification. The frequency of HSCs in sorted cells is determined using in vivo long-term marrow reconstitution assays, counting competitive repopulation units (CRUs) by limiting-dilution analysis. Purity of HSCs in the sorted fraction is estimated by dividing CRU frequency by seeding efficiency, a probability representing homing of tail-vein-infused HSCs to the bone marrow. The seeding efficiency of HSCs, like that of CFU-S (Siminovitch et al., 1963), was estimated to be between 10% and 20%, based on the 48 hr bone marrow seeding of cells capable of long-term reconstitution (Lanzkron et al., 1999). Using seeding efficiency as a "fudge factor," previous reports tended to overestimate the purity of HSCs in a given fraction. In 1996, however, Osawa et al. showed that transplantation of single $CD34^{low/negative}Kit^{+}Sca^{+}Lin^{-}$ ($CD34^{-}KSL$) cells into lethally irradiated congenic mice resulted in engraftment of 20% of the recipients, clearly indicating that the seeding efficiency must be higher than 20%. Single-cell transplantation experiments subsequently demonstrated engraftment rates of 30%–40% (Ema et al., 2000; Wagers et al., 2002), but the actual seeding efficiency of HSCs remained unclear.

In this issue, Matsuzaki et al. have demonstrated absolute engraftment of lethally irradiated syngenic recipients transplanted with sorted single HSCs from GFP-transgenic mice. While this study can be regarded as only another lap around the HSC-purification racetrack, it is a remarkable achievement, demonstrating over 95% long-term multilineage reconstitution after transplantation of a single purified HSC. The key to this success is six-color FACS analysis and cell sorting, using a combination of cell surface staining with monoclonal antibodies and Hoechst 33342 dye efflux analysis. The cells that have the strongest dye efflux capacity (Tip-SP cells), with a $CD34^{-}KSL$ phenotype, are HSCs with nearly 100% long-term marrow reconstitution capacity after single cell transplantation. One of three sets of experiments revealed long-term multilineage reconstitution in all 33 recipients after transplantation. The study proves that the marrow seeding efficiency of HSCs is nearly 100%.

These results highlight some intriguing features of HSCs. The efficiency of HSCs (among Tip-SP $CD34^{-}KSL$ cells) in seeding their bone marrow niche was nearly 100%, consistent with recent observations made by Iscove et al. (Benveniste et al., 2003). Based on these results, Matsuzaki et al. propose the capacity to home to bone marrow as a third criterion in defining HSCs. However, it may be too early to include homing capacity among the criteria for HSCs since it is not yet clear whether Tip-SP $CD34^{-}KSL$ cells constitute all HSCs in bone marrow. HSCs may exist that lack homing capacity and whose stem cell activity can be tested only by intrabone marrow injection. Perhaps HSCs and early hematopoietic progenitor cells differ simply in their ability to home to a bone marrow niche where HSCs can self-renew. This unexpectedly high homing capacity of HSCs is a significant and intriguing aspect of stem cell biology. Although osteoblastic cells reportedly have a role in the HSC bone marrow niche (Calvi et al., 2003; Zhang et al., 2003), not much is known about the site to which HSCs home. The molecular mechanisms regulating HSC homing deserve more intensive study, especially given the importance of such homing in a variety of medical applications.

The results here also may provide new insights into the debate about stem cell fate. Both stochastic and deterministic models have been proposed for the alternative fates of self-renewal versus lineage commitment. Till et al. suggested that stem cell fate is determined stochastically with an average frequency of ~60% for self-renewal (Till et al., 1964; Vogel et al., 1968). The findings of Matsuzaki et al. do not support this model; they favor the nonrandom, deterministic model. Because each transplanted single HSC reconstituted the recipient's bone marrow long-term, every individual HSC must have taken the path of self-renewal at the first cell division. Presumably, external signals promote this self-renewal.

The data of Matsuzaki et al. also implicate the cells with highest dye efflux capacity as the most primitive HSCs. Although Tip-SP $CD34^{-}KSL$ cells may not include all HSCs in the bone marrow, they represent a selected population for pure HSCs. Thus, at a minimum these

findings suggest a relationship among dye efflux capacity, repopulating capacity, and stem cell homing. Whether these stem cell functions are related to bcrp-1 (Zhou et al., 2001), a transporter responsible for the SP phenotype in HSCs and possibly other adult stem cells, poses a challenging question for stem cell biology.

Matsuzaki et al. have not only shown us how to isolate pure HSCs, which should aid studies of cell fate decision and stem cell regulation. They have provided important clues to understanding stem cell homing and the HSC niche.

Hideo Ema and Hiromitsu Nakauchi
Laboratory of Stem Cell Therapy
Center for Experimental Medicine
Institute of Medical Science
University of Tokyo
4-6-1 Shirokanedai, Minato-ku
Tokyo 108-8639
Japan

Selected Reading

Benveniste, P., Cantin, C., Hyam, D., and Iscove, N.N. (2003). Nat. Immunol. *4*, 708–713.

Calvi, L.M., Adams, G.B., Weibrecht, K.W., Weber, J.M., Olson, D.P., Knight, M.C., Martin, R.P., Schipani, E., Divieti, P., Bringhurst, F.R., et al. (2003). Nature *425*, 841–846.

Ema, H., Takano, H., Sudo, K., and Nakauchi, H. (2000). J. Exp. Med. *192*, 1281–1288.

Lanzkron, S.M., Collector, M.I., and Sharkis, S.J. (1999). Blood *93*, 1916–1921.

Matsuzaki, Y., Kinjo, K., Mulligan, R.C., and Okano, H. Immunity *20*, 87–93.

Osawa, M., Hanada, K.-i., Hamada, H., and Nakauchi, H. (1996). Science *273*, 242–245.

Siminovitch, L., McCulloch, E.A., and Till, J.E. (1963). J. Cell. Physiol. *62*, 327–336.

Till, J.E., McCulloch, E.A., and Siminovitch, L. (1964). Proc. Natl. Acad. Sci. USA *51*, 29–36.

Vogel, H., Niewisch, H., and Matioli, G. (1968). J. Cell. Physiol. *72*, 221–228.

Wagers, A.J., Sherwood, R.I., Christensen, J.L., and Weissman, I.L. (2002). Science *297*, 2256–2259.

Zhang, J., Niu, C., Ye, L., Huang, H., He, X., Tong, W.G., Ross, J., Haug, J., Johnson, T., Feng, J.Q., et al. (2003). Nature *425*, 836–841.

Zhou, S., Schuetz, J.D., Bunting, K.D., Colapietro, A.M., Sampath, J., Morris, J.J., Lagutina, I., Grosveld, G.C., Osawa, M., Nakauchi, H., et al. (2001). Nat. Med. *7*, 1028–1034.

Available online at www.sciencedirect.com
SCIENCE DIRECT®
Biochemical and Biophysical Research Communications 315 (2004) 356–362
BBRC
www.elsevier.com/locate/ybbrc

Roles of a conserved family of adaptor proteins, Lnk, SH2-B, and APS, for mast cell development, growth, and functions: *APS*-deficiency causes augmented degranulation and reduced actin assembly

Chiyomi Kubo-Akashi, Masanori Iseki, Sang-Mo Kwon, Hitoshi Takizawa, Kiyoshi Takatsu,* and Satoshi Takaki*

Division of Immunology, Department of Microbiology and Immunology, The Institute of Medical Science, The University of Tokyo, Shirokanedai 4-6-1, Minato-ku, Tokyo 108-8639, Japan

Received 18 December 2003

Abstract

Lnk, SH2-B, and APS form a conserved adaptor protein family. All of those proteins are expressed in mast cells and their possible functions in signaling through c-Kit or FcεRI have been speculated. To investigate roles of Lnk, SH2-B or APS in mast cells, we established IL-3-dependent mast cells from *lnk*$^{-/-}$, *SH2-B*$^{-/-}$, and *APS*$^{-/-}$ mice. IL-3-dependent growth of those cells was comparable. Proliferation or adhesion mediated by c-Kit as well as degranulation induced by cross-linking FcεRI were normal in the absence of Lnk or SH2-B. In contrast, *APS*-deficient mast cells showed augmented degranulation after cross-linking FcεRI compared to wild-type cells, while c-Kit-mediated proliferation and adhesion were kept unaffected. *APS*-deficient mast cells showed reduced actin assembly at steady state, although their various intracellular responses induced by cross-linking FcεRI were indistinguishable compared to wild-type cells. Our results suggest potential roles of APS in controlling actin cytoskeleton and magnitude of degranulation in mast cells.

Keywords: Actin cytoskeleton; Adaptor protein; BMMC; c-Kit; Cytokine; Cytokine receptor; Degranulation; FcεRI; IgE; Signal transduction; Tyrosine kinase

Mast cells play critical roles in allergic and inflammatory responses. Mast cells express the high affinity IgE receptor FcεRI and cross-linking of IgE bound to FcεRI by antigens initiates a series of molecular events in mast cells, which lead to degranulation and release of a wide variety of chemical mediators such as histamine, arachidonic acid metabolites, and soluble proteins including neutral proteases and cytokines [1–3]. Even in the absence of antigen, binding of monomeric IgE to FcεRI induces cytokine production and cell survival [4]. Mast cells differentiate from hematopoietic progenitor cells. Stem cell factor (SCF), which is also known as mast cell growth factor, and IL-3 provide signals for their differentiation, proliferation, and survival mediated through c-Kit receptor tyrosine kinase and IL-3 receptor, respectively. SCF also regulates chemotaxis and adhesion of mature mast cells [1,5].

Lnk, SH2-B, and APS form a conserved family of adaptor proteins, whose members share a homologous N-terminal region with proline rich stretches, PH and SH2 domains, and a conserved C-terminal tyrosine phosphorylation site [6–9]. Lnk plays a critical role in regulating production of B cell precursors and hematopoietic progenitor cells, and functions as a negative regulator of c-Kit-mediated signaling. We have shown that *lnk*$^{-/-}$ mice show enhanced B cell production because of the hypersensitivity of B cell precursors to SCF [8]. In addition, *lnk*$^{-/-}$ mice exhibit increased numbers of hematopoietic progenitors in the bone marrow, and the ability of hematopoietic progenitors to repopulate

* Corresponding authors. Fax: +81-3-5449-5407.
E-mail addresses: takatsuk@ims.u-tokyo.ac.jp (K. Takatsu), takakis@ims.u-tokyo.ac.jp (S. Takaki).

0006-291X/$ - see front matter © 2004 Elsevier Inc. All rights reserved.
doi:10.1016/j.bbrc.2004.01.060

irradiated host animals was greatly enhanced by the absence of Lnk [10]. Independently, Velazquez et al. [11] have reported *lnk*-deficiency results in abnormal modulation of SCF and IL-3-mediated signaling pathways and augmented growth of bone marrow cells or splenocytes. SH2-B is originally identified as a protein associated with immunoreceptor tyrosine-based activation motifs (ITAMs) of FcεRI γ-chain by a modified two-hybrid (tribrid system) screening [6]. We have shown that SH2-B is a critical molecule for the maturation of reproduction organs that is at least in part mediated by insulin-like growth factor I (IGF-I) receptor signaling [12]. APS is identified as a potential substrate of c-Kit by two-hybrid system [7]. We also independently isolated the murine counterpart of APS as a protein homologous to Lnk and SH2-B [9]. APS is phosphorylated upon stimulation with various growth factors, including EPO-R, PDGF-R, insulin, nerve growth factor (NGF), and cross-linking B cell receptor (BCR) [9,13–16]. Recently, we generated *APS*$^{-/-}$ mice and found that B-1 cells in peritoneal cavity were increased, and humoral immune responses to type-2 antigen significantly enhanced in *APS*$^{-/-}$ mice [17].

Lnk-family adaptor proteins, Lnk, SH2-B, and APS, are all expressed in bone marrow-derived mast cells (BMMCs) [12]. In addition, various experiments using cell lines overexpressing those Lnk-family adaptor proteins suggested their possible functions in signaling mediated through c-Kit or FcεRI. We investigated and compared for the first time consequences of the deficiency either of Lnk, SH2-B or APS in mast cell functions using primary cultured cells. We established BMMCs from bone marrow progenitors of *lnk*$^{-/-}$, *SH2-B*$^{-/-}$, *APS*$^{-/-}$ mice, and their respective control wild-type mice. IL-3-dependent BMMCs were equally established even in the absence of Lnk, SH2-B or APS. SCF-dependent proliferation or adhesion was also not compromised and was comparable among *lnk*$^{-/-}$, *SH2-B*$^{-/-}$, and *APS*$^{-/-}$ BMMCs. Although FcεRI-mediated degranulation was not affected by the absence of Lnk or SH2-B, *APS*$^{-/-}$ BMMCs showed enhanced degranulation after cross-linking FcεRI. *APS*$^{-/-}$ BMMCs showed reduced filamentous actin (F-actin) assembly at steady state and was resistant to inhibitors disrupting F-actin microfilaments in FcεRI-mediated degranulation responses. These results suggest that APS plays a role in negative regulation of mast cell degranulation by controlling actin dynamics.

Materials and methods

Cells and culture. Bone marrow cells were obtained from 8- to 10-week-old *lnk*$^{-/-}$ [8], *SH2-B*$^{-/-}$ [12], *APS*$^{-/-}$ mice [17], and their respective wild-type littermates, and cultured in RPMI1640 supplemented with 5 ng/ml murine IL-3 (PeproTech), 8% fetal calf serum (FCS), nonessential amino acids (Gibco-BRL), 100 IU/ml penicillin, 100 μg/ml streptomycin, and 10 μM of 2-mercaptoethanol. Cells were split and supplied with fresh medium every 4 or 5 days. After 4 weeks of cultivation, greater than 95% of cells were c-Kit and FcεRI positive as assessed by flow cytometry.

Flow cytometry and cytochemistry. For the detection of FcεRI, BMMCs were incubated in a supernatant of IGEL a2 (15.3) hybridoma containing mouse anti-DNP IgE monoclonal antibody (mAb) and then stained with fluorescein isothiocyanate (FITC)-conjugated anti-mouse IgE mAb (LO-ME-2, Oxford Biomarketing, UK). For the detection of c-Kit, cells were stained with phycoerythrin (PE)-conjugated anti-CD117 mAb (2B8, Pharmingen). For measurements of F-actin content, cells were fixed in 3.7% formaldehyde for 6 h at 4 °C permeabilized with 0.2% Triton X-100 in PBS for 30 min and then stained with rhodamine-conjugated phalloidin (Molecular Probes, Eugene, OR) for 1 h. Stained cells were then analyzed by flow cytometry using a FACSCalibur (Becton–Dickinson).

Unstimulated or stimulated BMMCs were resuspended in PBS and deposited onto microscope slides using a Cytospin 3 (Shandon Scientific, Cheshire, England). After staining with May–Gruenwald's and Giemsa's solutions (MERCK), cellular morphology was assessed by a light microscope.

Proliferation and survival assays. BMMCs (5×10^4) were cultured in 0.2 ml of flesh medium containing various concentrations of SCF (PeproTech) in a 96-well multi-well plate for 72 h. Cells were pulsed with [^{3}H]thymidine (0.2 μCi/well) in the last 12 h of culture and harvested and incorporated [^{3}H]thymidine was measured in triplicate determination using a MATRIX 96 Direct Beta Counter (Packard, Meriden, CT). Cells were cultured in media alone or in the presence of various concentrations of anti-DNP IgE mAb (SPE-7, Sigma). Percentage of viable cells was determined by trypan blue exclusion.

Adhesion assay. Adhesion assays to fibronectin were performed as previously described [18]. In brief, 5×10^4 BMMCs labeled with 2′,7′-bis-(2-carboxyethyl)-5-(and-6)-carboxy fluorescein (BCECF: Molecular Probes, Eugene, OR) were incubated in triplicate in a 96-well polystyrene plate (Lynbro-Titertek, Aurora, OH) coated with fibronectin (Sigma) in the presence of various concentrations of SCF or 10 ng/ml PMA at 37 °C for 30 min. Unbound cells were removed by washing the plates with binding medium RPMI 1640 containing 10 mM Hepes (pH 7.4), and 0.03% BSA four times. Adhered cells were quantified by measuring fluorescence of input and bound cells using a Fluorescence Concentration Analyzer (IDEXX Laboratories, Westbrook, ME).

Degranulation assay. BMMCs were sensitized with anti-DNP IgE at 37 °C for 18 h, washed, and resuspended in Tyrode's buffer (10 mM Hepes, pH 7.4, 130 mM NaCl, 5 mM KCl, 1.4 mM $CaCl_2$, 1 mM $MgCl_2$, 5.6 mM glucose, and 0.1% BSA). Cells (5×10^5 in 0.2 ml) were then stimulated with various concentrations of DNP-BSA or 10 ng/ml PMA plus 400 ng/ml ionomycin at 37 °C for 1 h. Enzymatic activities of β-hexosaminidase in supernatants and cells solubilized in 0.5% Triton X-100 Tyrode's buffer were measured using *p*-nitrophenyl *N*-acetyl-β-D-glucosaminidase (Sigma) as substrates. Degranulation was calculated as the percentage of β-hexosaminidase released from cells in the total amount of the enzyme in the supernatants and cell pellets as described before [18]. For the experiment using latrunculin, sensitized BMMCs were pretreated with various concentrations of latrunculin for 15 min at 37 °C before assays. Histamine released into culture supernatants after degranulation was measured using ELISA kit (Immunotech, Marseille, France) according to manufacturer's recommendation.

Calcium measurements. Sensitized BMMCs were incubated with 6 μM Fura PE3/AM (TEFLABS, Austin, TX) in PBS containing 20 mM Hepes (pH 7.4), 5 mM glucose, 0.025% BSA, and 1 mM $CaCl_2$ (HBS) at 37 °C for 60 min. Cells were washed and resuspended in HBS (1×10^5 cells/0.1 ml) in a stirring cuvette. Fluorescence was monitored continuously with a fluorescence spectrophotometer (CAF-110: JASCO, Osaka, Japan) at an emission wavelength of 500 nm and two different excitation wavelengths (340 and 380 nm).

Immunoblotting. Cell lysates from stimulated BMMCs were subjected to immunoprecipitation and Western blot analysis as previously

described [9]. The proteins were resolved by SDS–8% PAGE and transferred to PVDF membranes (Immobilon, Millipore). After blocking with 5% BSA, membranes were probed with anti-phosphotyrosine mAb (4G10, Upstate Biotechnology) and incubated with HRP-conjugated secondary antibodies. Blots were washed in 0.05% Tween 20/Tris-buffered saline, pH 7.6, and proteins were detected by chemiluminescence (Perkin–Elmer Life Sciences).

Results

Establishment of BMMCs lacking either Lnk, SH2-B or APS

Lnk, SH2-B, and APS were all expressed in normal BMMCs [12]. To investigate possible functions of those adaptor proteins in mast cells, we established IL-3-dependent BMMCs from bone marrow progenitors of *lnk*$^{-/-}$, *SH2-B*$^{-/-}$, and *APS*$^{-/-}$ mice and their responses were compared with those of BMMCs established from respective control wild-type littermates. IL-3-dependent growth of *lnk*$^{-/-}$, *SH2-B*$^{-/-}$ or *APS*$^{-/-}$ bone marrow progenitor cells was almost comparable to that of respective control progenitor cells (Fig. 1A). Established *lnk*$^{-/-}$, *SH2-B*$^{-/-}$ or *APS*$^{-/-}$ BMMCs were not distinguishable from the wild-type BMMCs in terms of surface expression of FcεRI and c-Kit (Fig. 1B). Mast cell differentiation and proliferation induced by IL-3 was not affected at all even in the absence of Lnk, SH2-B or APS.

Functions of lnk$^{-/-}$, *SH2-B*$^{-/-}$ *or APS*$^{-/-}$ *BMMCs*

First, we examined proliferative responses of established BMMCs to SCF and found no difference among *lnk*$^{-/-}$, *SH2-B*$^{-/-}$, *APS*$^{-/-}$, and respective control BMMCs (Fig. 2A). Adhesion to fibronectin induced by SCF or PMA was also not affected in the absence of Lnk, SH2-B or APS (Fig. 2B). We then examined degranulation of those BMMCs induced by cross-linking FcεRI by measuring β-hexosaminidase and histamine released after stimulation. Degranulation from *lnk*$^{-/-}$ or *SH2-B*$^{-/-}$ BMMCs was almost comparable to that from control wild-type BMMCs (Fig. 2C). In contrast, *APS*$^{-/-}$ BMMCs showed enhanced degranulation responses upon cross-linking FcεRI (Fig. 2C). Degranulation from *APS*$^{-/-}$ BMMCs, determined by β-hexosaminidase releasability, was 130–140% of that from control cells at each stimulation condition, and the enhancement was statistically significant at the concentrations of DNP-BSA over 0.5 μg/ml (Table 1). Histamine released after cross-linking FcεRI was also augmented in *APS*$^{-/-}$ BMMCs (data not shown).

FcεRI-mediated cellular responses in APS$^{-/-}$ *BMMCs*

To clarify the possible molecular mechanisms leading to the enhanced degranulation in the absence of APS,

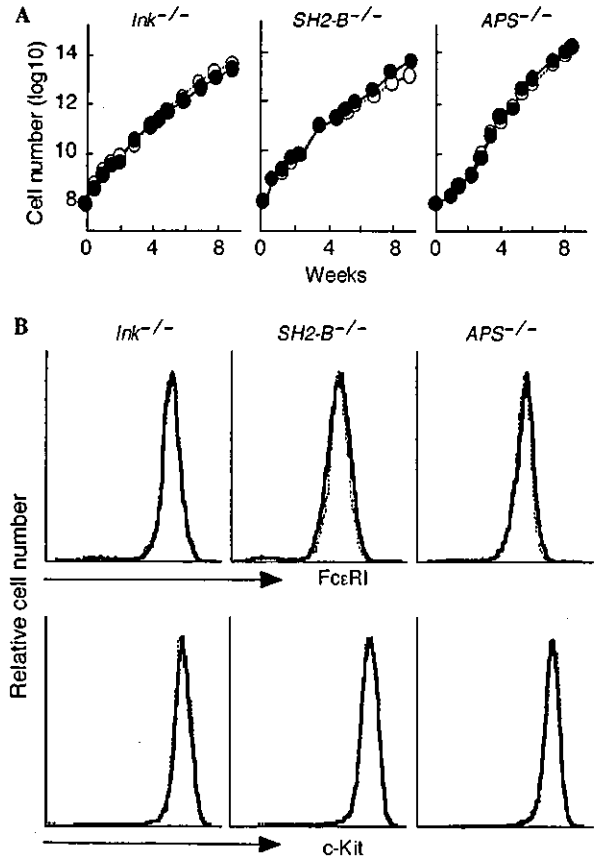

Fig. 1. (A) Cumulative cell numbers of *lnk*$^{-/-}$, *SH2-B*$^{-/-}$, *APS*$^{-/-}$ (closed circles), and respective wild-type control (open circles) BMMCs. Differentiation of BMMCs from progenitors and their cell growth induced by IL-3 was comparable in the absence of either Lnk, SH2-B or APS. Representative results obtained from multiple independent pairs of BMMCs are shown. (B) Surface expressions of FcεRI (upper panels) or c-Kit (lower panels) on *lnk*$^{-/-}$, *SH2-B*$^{-/-}$, *APS*$^{-/-}$ (bold lines), and respective wild-type control (dotted lines) BMMCs. After IgE sensitization, BMMCs were stained with anti-c-Kit or anti-IgE antibodies and analyzed by flow cytometry. Representative results of multiple independent experiments are shown.

we tried to evaluate various cellular events induced by cross-linking FcεRI. We first cytochemically evaluated the proportion of degranulated BMMCs after stimulation. Percentage of degranulated cells increased in a dose-dependent manner as the concentration of antigens increased. Importantly, the ratio of degranulated BMMCs in each stimulation condition was comparable between *APS*$^{-/-}$ and wild-type BMMCs (Fig. 3A). The enhanced degranulation from *APS*$^{-/-}$ BMMCs was thus due to augmented degranulation from each mast cell but not to increased proportion of cells that underwent degranulation. We then analyzed calcium influx induced by cross-linking FcεRI, however, we did not observe significant difference in initial peak and following sustained increase of intracellular free calcium between *APS*$^{-/-}$ and control BMMCs (Fig. 3B). Cell survival

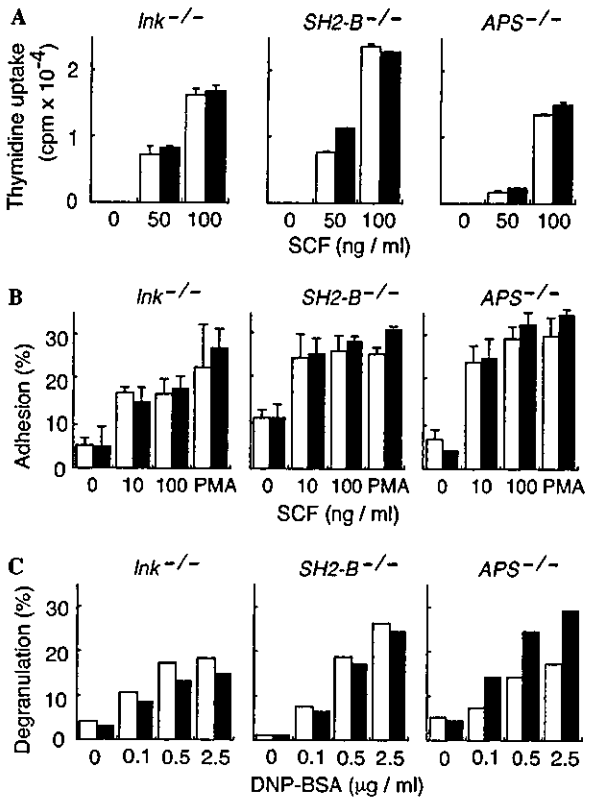

Fig. 2. Responses of *lnk*$^{-/-}$, *SH2-B*$^{-/-}$ or *APS*$^{-/-}$ BMMCs (filled bars) and of respective control BMMCs (open bars) induced by activation of c-Kit or FcεRI. (A) Proliferation upon stimulation with various concentrations of SCF. Values shown are the mean cpm ± SD of triplicate determinations. (B) Adhesion to fibronectin induced by various concentrations of SCF or 10 ng/ml PMA. Shown are average ± SD of triplicate measurements. (C) Degranulation after cross-linking FcεRI. Cells sensitized with anti-DNP IgE mAb were stimulated with the various concentrations of DNP-BSA. Shown is the percentage of β-hexosaminidase activity released into culture supernatants out of the total β-hexosaminidase initially stored in cells. *APS*$^{-/-}$ BMMCs showed augmented degranulation responses (see also Table 1). Representative results of three independent experiments are shown from (A) through (C).

mediated by binding of monomeric IgE to FcεRI was also comparable (Fig. 3C). Tyrosine phosphorylation of various cellular proteins was rapidly induced after cross-linking FcεRI in mast cells and was comparable between *APS*$^{-/-}$ and wild-type BMMCs. Phosphorylation of neither Akt nor PKCδ molecules was affected in the absence of APS (data not shown).

Decreased actin assembly in APS$^{-/-}$ *BMMCs*

It has been shown that Lnk associates with an actin binding protein ABP-280 [19] and that SH2-B plays a role in actin reorganization and cell motility mediated by growth hormone receptor [20,21]. We recently found that Lnk facilitates actin reorganization in transfected fibroblast cells (S.M.K. and S.T., unpublished data). In addition, a negative correlation between actin polymerization and FcεRI-mediated degranulation from RBL-2H3 mast cell line has been presented [22,23].

We speculated APS may regulate actin cytoskeleton, which potentially has regulatory process for degranulation in mast cells. Therefore, we investigated consequences of inhibition of actin polymerization induced by cross-linking FcεRI in BMMCs and its effect on degranulation by treatment with latrunculin. Treatment of sensitized BMMCs with latrunculin resulted in the reduction of F-actin contents as demonstrated by rhodamine–phalloidine binding (Fig. 4A, left panel). Cross-linking FcεRI induced reduction of F-actin contents in stimulated BMMCs. Consistent with observations using RBL-2H3 cells, inhibition of actin assembly by treatment with latrunculin enhanced degranulation from normal BMMCs in a dose-dependent manner (Fig. 4A, right). Interestingly, sensitized *APS*$^{-/-}$ BMMCs showed reduced F-actin content (about 70% of control) compared to wild-type cells (Fig. 4B, left). The reduction in F-actin contents became less evident in cells treated with latrunculin. Finally, the effect of latrunculin on degranulation was compared between *APS*$^{-/-}$ and control BMMCs. As shown in Fig. 4B, augmented degranulation by *APS*$^{-/-}$ BMMCs became less evident by treatment with latrunculin, which was well correlated with difference in F-actin contents between latrunculin treated *APS*$^{-/-}$ and control cells. These results suggested that *APS*-deficiency in mast cells made actin assembly at relatively low levels and that resulted in facilitated degranulation process after cross-linking FcεRI.

Table 1
Enhancement of FcεRI-induced degranulation in *APS*$^{-/-}$ BMMC

DNP-BSA(μg/ml)	Degranulation (% maximal response induced by PMA plus ionomycin)			
	0	0.1	0.5	2.5
+/+ ($n = 11$)	5.6 ± 0.9	19.4 ± 2.4	28.9 ± 2.5	29.4 ± 2.1
−/− ($n = 11$)	5.0 ± 0.7	25.8 ± 3.9	39.5 ± 3.9*	40.6 ± 3.4**
(% +/+ response)	(89%)	(133%)	(136%)	(138%)

Sensitized BMMCs were stimulated with the various concentrations of DNP-BSA or 10 ng/ml PMA plus 400 ng/ml ionomycin. Values represent the mean ± SE of % β-hexosaminidase activity normalized by the value induced with PMA plus ionomycin as 100%. *$p < 0.05$, **$p < 0.01$ compared to +/+ BMMCs by Student's t test.

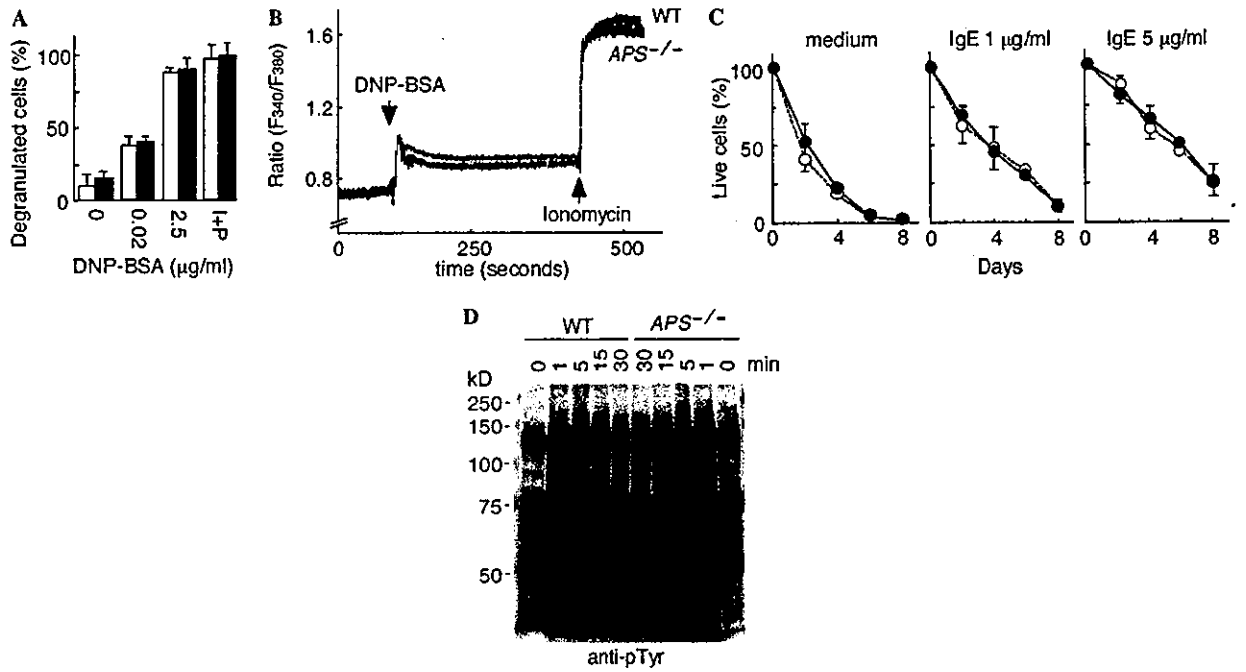

Fig. 3. Cellular responses of $APS^{-/-}$ BMMCs mediated through cross-linking FcεRI. (A) Proportion of degranulated cells after cross-linking FcεRI with various concentrations of antigens was determined by cytochemistry. Percentages of degranulated cells were comparable between $APS^{-/-}$ (closed bars) and wild-type control mice (open bars). The average ± SD of three independent experiments are shown. (B) Calcium influx induced upon cross-linking FcεRI in $APS^{-/-}$ (lower line) and wild-type (upper line) BMMCs. After IgE sensitization, BMMCs were loaded with Fura PE3 and stimulated with 5 μg/ml DNP-BSA and 10 μg/ml ionomycin at the indicated time points (arrows), and fluorescence intensity ratio at 340–380 nm was measured. Representative results of two independent experiments are shown. (C) Survival of $APS^{-/-}$ (closed circles) and wild-type (open circles) BMMCs by binding of monomeric IgE to FcεRI. Cells were cultivated in the absence or in the presence of various concentrations of monomeric IgE and percentages of live cells were measured. The average ± SD of three independent experiments are shown. (D) Tyrosine phosphorylation of total cellular proteins after cross-linking FcεRI. Sensitized BMMCs were stimulated with 2.5 μg/ml DNP-BSA for the indicated times. Total cell lysates were separated through SDS–PAGE and subjected to immunoblot using anti-phosphotyrosine mAb (4G10). Representative results of three experiments are shown.

Discussion

We investigated functions of Lnk, SH2-B or APS in mast cells, since possible regulatory roles of Lnk-family adaptor proteins in signaling through c-Kit or FcεRI had been suggested. We established BMMCs lacking either Lnk, SH2-B or APS and examined their cellular responses. None of those mutant BMMCs showed altered responses against IL-3 or SCF, the c-Kit ligand. *APS*-deficiency resulted in enhanced FcεRI-mediated degranulation, while both $lnk^{-/-}$ and $SH2\text{-}B^{-/-}$ BMMCs did not show any abnormal responses induced by cross-linking FcεRI.

We have shown that Lnk negatively regulates c-Kit signaling in B cell precursors and hematopoietic progenitor cells [8,10]. We did not observe significant enhancement in SCF-dependent growth of $lnk^{-/-}$ BMMCs in contrast to a previous report by Velazquez et al. [11]. SCF-dependent adherence was also comparable to normal cells. Expression levels of *lnk* transcripts are rather low in BMMCs compared to B-lineage cells or hematopoietic progenitor cells (unpublished data). It is likely that *lnk*-deficiency alone hardly affects mast cell function because of low expression of Lnk in mast cells.

APS had been cloned as a possible candidate substrate for the c-Kit [7]. However, $APS^{-/-}$ BMMCs did not show any altered responses upon stimulation with SCF. Instead, they showed enhanced FcεRI-mediated degranulation. $APS^{-/-}$ BMMCs showed reduced actin assembly at steady state compared to normal BMMCs. Inhibition of actin assembly in normal BMMCs by latrunculin resulted in enhanced degranulation similar to $APS^{-/-}$ BMMCs. In $APS^{-/-}$ mice, B-1 cells in peritoneal cavity increased and showed reduced F-actin contents. Conversely, in transgenic mice overexpressing APS in lymphocytes, B cells were reduced and showed enhanced actin assembly [17]. These results suggest that APS may negatively regulate degranulation process by controlling actin dynamics in mast cells. In RBL-2H3 mast cells, F-actin assembly induced by cross-linking FcεRI negatively controls degranulation as well as calcium signaling [22,23]. Oka et al. [24] recently reported that monomeric IgE binding induced actin assembly and that inhibition

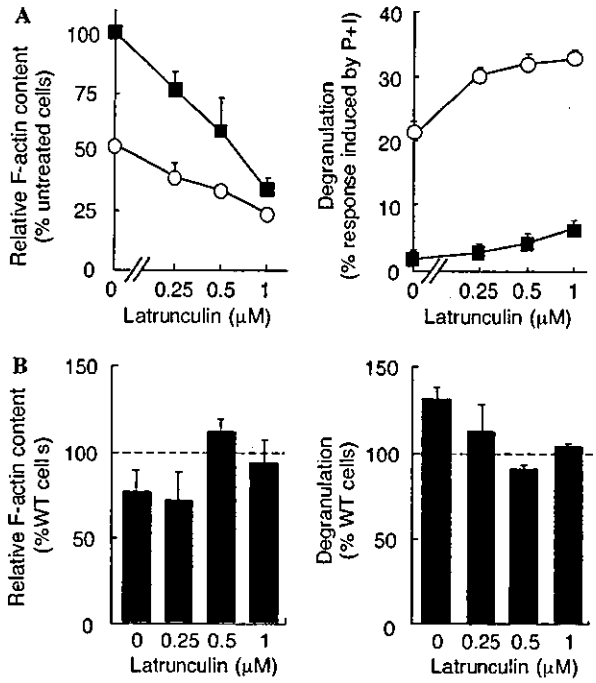

Fig. 4. Enhanced degranulation correlated with reduced F-actin contents in BMMCs treated with inhibitor of actin assembly, latrunculin or by APS-deficiency. (A) Treatment with latrunculin inhibited actin assembly and resulted in reduced F-actin content in BMMCs. Sensitized wild-type BMMCs were incubated with the various concentrations of latrunculin, kept unstimulated (squares) or stimulated with 2.5 μg/ml DNP-BSA (circles). F-actin contents of cells were then analyzed by rhodamine–phalloidin staining and flow cytometry, and the results are shown as relative F-actin contents compared with that of unstimulated cells in the absence of latrunculin (left). Degranulation was determined by measuring β-hexosaminidase activity released into culture supernatants, and results were shown as percent maximal responses induced by PMA and ionomycin treatment (right). (B) F-actin content of *APS*$^{-/-}$ BMMCs in the absence or the presence of various concentrations of latrunculin was measured and relative F-actin contents compared with those of control cells treated with the same concentrations of latrunculin were shown (left). Degranulation from *APS*$^{-/-}$ BMMCs treated with latrunculin was measured, and shown as percent reaction compared with those from wild-type control cells in the same conditions (right). Results shown are means ± SE of values obtained from three independent experiments.

of IgE-induced actin assembly by cytochalasin D initiates calcium influx and degranulation. Although enhancement of calcium influx in *APS*$^{-/-}$ BMMCs was not observed, reduction of actin assembly in *APS*$^{-/-}$ BMMCs may lead to augmented degranulation in analogy with those observed in RBL-2H3 mast cells. The molecular mechanisms for APS-mediated actin assembly as well as APS function downstream of cross-linking FcεRI remain to be elucidated.

APS function in insulin-R signaling has been also indicated in various experiments using cell lines [15,16,25–27]. *APS*$^{-/-}$ mice exhibited increased sensitivity to insulin and enhanced glucose tolerance [28]. It is intriguing to examine whether effect of *APS*-deficiency on insulin sensitivity is also mediated by actin dynamics. Regulation of actin cytoskeleton seems one of the common functions of Lnk-family adaptor proteins. Lnk associates with an actin binding protein ABP-280 [19] and facilitates actin assembly in overexpressed fibroblasts by activating Vav and Rac (S.M.K. and S.T., unpublished data). SH2-B is required for actin reorganization and regulates cell motility induced by GH-R activation [20,21].

SH2-B has been identified as a possible adaptor binding to ITAMs of FcεRI γ chain [6]. However, all examined responses induced by FcεRI ligation were normal with *SH2-B*$^{-/-}$ *BMMCs*. It seems *SH2-B*-deficiency do not affect mast cell function. However, it should be notified that interaction of SH2 domains of Lnk-family proteins with c-Kit or ITAM of FcεRI γ chain had been demonstrated in overexpression systems with different combinations, for example, SH2-B with FcεRI γ chain, APS with c-Kit. *SH2-B*$^{-/-}$ mice showed mild growth retardation and infertility due to impaired maturation of gonad organs [12]. Thus, SH2-B seemed to have a true target except FcεRI, worked as a positive regulator of signal transduction in contrast to Lnk and APS that function as negative regulators as shown in previous studies and in this study. Despite the significant structural similarities between APS, Lnk, and SH2-B, their functions appear to be quite different from each other. However, possible common functions of those adaptor proteins in vivo should be examined by generating mutant mice lacking APS, Lnk or SH2-B in various combinations.

In conclusion, our studies describe roles of Lnk family adaptor proteins on BMMCs. Both Lnk and SH2-B were dispensable for various mast cell responses mediated through c-Kit, FcεRI as well as IL-3-R. APS plays a role in controlling FcεRI-induced degranulation response but not in c-Kit-mediated proliferation or adhesion. APS may regulate degranulation by controlling actin dynamics in mast cells.

Acknowledgments

We thank our colleagues for helpful discussions, technical advices, and critical reading of the manuscript. This work was performed through Special Coordination Funds for Promoting Science and Technology, and Grants-in-Aid from the Ministry of Education, Culture, Sports, Science and Technology, the Japanese Government.

References

[1] D.D. Metcalfe, D. Baram, Y.A. Mekori, Mast cells, Physiol. Rev. 77 (1997) 1033–1079.
[2] S.J. Galli, Mast cells and basophils, Curr. Opin. Hematol. 7 (2000) 32–39.
[3] J. Rivera, Molecular adapters in Fc(epsilon)RI signaling and the allergic response, Curr. Opin. Immunol. 14 (2002) 688–693.

[4] J. Kalesnikoff, M. Huber, V. Lam, J.E. Damen, J. Zhang, R.P. Siraganian, G. Krystal, Monomeric IgE stimulates signaling pathways in mast cells that lead to cytokine production and cell survival, Immunity 14 (2001) 801–811.
[5] K. Vosseller, G. Stella, N.S. Yee, P. Besmer, c-kit receptor signaling through its phosphatidylinositide-3′-kinase-binding site and protein kinase C: role in mast cell enhancement of degranulation, adhesion, and membrane ruffling, Mol. Biol. Cell. 8 (1997) 909–922.
[6] M.A. Osborne, S. Dalton, J.P. Kochan, The yeast tribrid system: genetic detection of trans-phosphorylated ITAM-SH2-interactions, Biotechnology 13 (1995) 1474–1478.
[7] M. Yokouchi, R. Suzuki, M. Masuhara, S. Komiya, A. Inoue, A. Yoshimura, Cloning and characterization of APS, an adaptor molecule containing PH and SH2 domains that is tyrosine phosphorylated upon B-cell receptor stimulation, Oncogene 15 (1997) 7–15.
[8] S. Takaki, K. Sauer, B.M. Iritani, S. Chien, Y. Ebihara, K. Tsuji, K. Takatsu, R.M. Perlmutter, Control of B cell production by the adaptor protein Lnk: definition of a conserved family of signal-modulating proteins, Immunity 13 (2000) 599–609.
[9] M. Iseki, S. Takaki, K. Takatsu, Molecular cloning of the mouse APS as a member of the Lnk family adaptor proteins, Biochem. Biophys. Res. Commun. 272 (2000) 45–54.
[10] S. Takaki, H. Morita, Y. Tezuka, K. Takatsu, Enhanced hematopoiesis by hematopoietic progenitor cells lacking intracellular adaptor protein, Lnk, J. Exp. Med. 195 (2002) 151–160.
[11] L. Velazquez, A.M. Cheng, H.E. Fleming, C. Furlonger, S. Vesely, A. Bernstein, C.J. Paige, T. Pawson, Cytokine signaling and hematopoietic homeostasis are disrupted in Lnk-deficient mice, J. Exp. Med. 195 (2002) 1599–1611.
[12] S. Ohtsuka, S. Takaki, M. Iseki, K. Miyoshi, N. Nakagata, Y. Kataoka, N. Yoshida, K. Takatsu, A. Yoshimura, SH2-B is required for both male and female reproduction, Mol. Cell. Biol. 22 (2002) 3066–3077.
[13] M. Yokouchi, T. Wakioka, H. Sakamoto, H. Yasukawa, S. Ohtsuka, A. Sasaki, M. Ohtsubo, M. Valius, A. Inoue, S. Komiya, A. Yoshimura, APS, an adaptor protein containing PH and SH2 domains, is associated with the PDGF receptor and c-Cbl and inhibits PDGF-induced mitogenesis, Oncogene 18 (1999) 759–767.
[14] X. Qian, A. Riccio, Y. Zhang, D.D. Ginty, Identification and characterization of novel substrates of Trk receptors in developing neurons, Neuron 21 (1998) 1017–1029.
[15] Z. Ahmed, B.J. Smith, K. Kotani, P. Wilden, T.S. Pillay, APS, an adapter protein with a PH and SH2 domain, is a substrate for the insulin receptor kinase, Biochem. J. 341 (1999) 665–668.
[16] S.A. Moodie, J. Alleman-Sposeto, T.A. Gustafson, Identification of the APS protein as a novel insulin receptor substrate, J. Biol. Chem. 274 (1999) 11186–11193.
[17] M. Iseki, C. Kubo, S.M. Kwon, A. Yamaguchi, Y. Kataoka, N. Yoshida, K. Takatsu, S. Takaki, Increased numbers of B-1 cells and enhanced responses against TI-2 antigen in mice lacking APS, an adaptor molecule containing PH and SH2 domains, Mol. Cell. Biol. 24 (2004) in press.
[18] R. Setoguchi, T. Kinashi, H. Sagara, K. Hirosawa, K. Takatsu, Defective degranulation and calcium mobilization of bone-marrow derived mast cells from Xid and Btk-deficient mice, Immunol. Lett. 64 (1998) 109–118.
[19] X. He, Y. Li, J. Schembri-King, S. Jakes, J. Hayashi, Identification of actin binding protein, ABP-280, as a binding partner of human Lnk adaptor protein, Mol. Immunol. 37 (2000) 603–612.
[20] J. Herrington, M. Diakonova, L. Rui, D.R. Gunter, C. Carter-Su, SH2-B is required for growth hormone-induced actin reorganization, J. Biol. Chem. 275 (2000) 13126–13133.
[21] M. Diakonova, D.R. Gunter, J. Herrington, C. Carter-Su, SH2-Bβ is a Rac-binding protein that regulates cell motility, J. Biol. Chem. 277 (2002) 10669–10677.
[22] L. Frigeri, J.R. Apgar, The role of actin microfilaments in the down-regulation of the degranulation response in RBL-2H3 mast cells, J. Immunol. 162 (1999) 2243–2250.
[23] T. Oka, K. Sato, M. Hori, H. Ozaki, H. Karaki, Fc epsilonRI cross-linking-induced actin assembly mediates calcium signalling in RBL-2H3 mast cells, Br. J. Pharmacol. 136 (2002) 837–846.
[24] T. Oka, M. Hori, A. Tanaka, H. Matsuda, H. Karaki, H. Ozaki, IgE alone-induced actin assembly modifies calcium signaling and degranulation in RBL-2H3 mast cells, Am. J. Physiol. Cell Physiol. 17 (2003) 17.
[25] Z. Ahmed, B.J. Smith, T.S. Pillay, The APS adapter protein couples the insulin receptor to the phosphorylation of c-Cbl and facilitates ligand-stimulated ubiquitination of the insulin receptor, FEBS Lett. 475 (2000) 31–34.
[26] Z. Ahmed, T.S. Pillay, Functional effects of APS and SH2-B on insulin receptor signalling, Biochem. Soc. Trans. 29 (2001) 529–534.
[27] J. Liu, A. Kimura, C.A. Baumann, A.R. Saltiel, APS facilitates c-Cbl tyrosine phosphorylation and GLUT4 translocation in response to insulin in 3T3-L1 adipocytes, Mol. Cell. Biol. 22 (2002) 3599–3609.
[28] A. Minami, M. Iseki, K. Kishi, M. Wang, M. Ogura, N. Furukawa, S. Hayashi, M. Yamada, T. Obata, Y. Takeshita, Y. Nakaya, Y. Bando, K. Izumi, S.A. Moodie, F. Kajiura, M. Matsumoto, K. Takatsu, S. Takaki, Y. Ebina, Increased insulin sensitivity and hypoinsulinemia in APS knockout mice, Diabetes 52 (2003) 2657–2665.

別紙４

研究成果の刊行に関する一覧表

書籍

著者氏名	論文タイトル名	書籍全体の編集者名	書　籍　名	出版社名	出版地	出版年	ページ
Ema H, Morita Y and Nakauchi H.	Phenotype of mouse hematopoietic stem cells.	Lanza R, Blau H, Melton D, Moore M, Thomas ED, Verfaillie C., Weissman I, West M	*Handbook of Stem Cells*	Elsevier Academic Press Inc.	U.S.A.	2004	323-328

雑誌

発表者氏名	論文タイトル名	発表誌名	巻号	ページ	出版年
Kaneko S, Nagasawa T, Nakauhi H, and Onodera M.	An in vivo assay for retrovirally transduced human peripheral T lymphocytes using nonobese diabetic/severe combined immunodeficiency mice.	*Exp. Hematology,*	33	35-41	2005
Ema H, Sudo K, Seita J, Maeda A, Osawa M, Takatsu K, Takaki S, and Nakauchi H.	Quantification of self-renewal capacity in single hematopoietic stem cells from normal and Lnk-deficient mice.	*Developmental Cell.*		In press	2005
Iwama A, Oguro H, Negishi M, Kato Y, Morita Y, Tsukui H, Ema H, Kamijo T, Katoh-Fukui Y, Koseki H, Lohuizen van M, and Nakauchi H.	Enhanced self-renewal of hematopoietic stem cells mediated by the polycomb gene product, Bmi-1.	*Immunity.*	21	843-851	2004
Yasuda T, Shirakata M, Iwama A, Ishii A, Ebihara Y, Osawa M, Honda K, Shinohara H, Sudo K, Tsuji K, Nakauchi H, Iwakura Y, Hirai H, Oda H, Yamamoto T. and Yuji Yamanashi.	Role of Dok-1 and Dok-2 in myeloid homeostasis and suppression of leukemia. *J. Exp. Med.*	*J Exp Med.*	20	1681-1687	2004

Ojima K, Uezumi A, Miyoshi H, Masuda S, Morita Y. Fukase A, Hattori A, Nakauchi H,	Miyagoe-Suzuki Y, Kakeda S. Mac-1^{low} early myeloid cells in the bone marrow-derived SP fraction migrate into injured skeletal muscle and participate in muscle regenaration.	*Biochemmical and Biophysical Research Comunications.*	321	1051-1060	2004
Takano H, Ema H, Nakauchi H.	Asymmetric division and lineage commitment at the level of hematopoietic stem cells: inference from differentiation in daughter cell and granddaughter cell pairs.	*J Exp Med*	199	295-302	2004
Ema H, Nakauchi H.	"Homing to Niche," a new criterion for hematopoietic stem cells?	*Immunity*	20	1-2	2004
Sumazaki R, Shiojiri N, Isoyama S, Masu M, Keino-Masu K, Osawa M, Nakauchi H, Kageyama R, Matsui A.	Conversion of biliary system to pancreatic tissue in Hesl-deficient mice.	*Nat Genet*	6	83-7	2004
Suzuki A, Nakauchi H, Taniguchi H.	Prospective isolation of multipotent pancreatic progenitors using flow-cytometric cell sorting.	*Diabetes.*	53	2143-52	2004
Miyagi S, Saito T, Mizutani K, Masuyama N, Gotoh Y, Iwama A, Nakauchi H, Masui S, Niwa H, Nishimoto M, Muramatsu M, Okuda A.	The Sox-2 regulatory regions display their activities in two distinct types of multipotent stem cells.	*Mol Cell Biol.*	24	4207-20	2004
Suzuki A, Zheng YW, Fukao K, Nakauchi H, Taniguchi H.	Liver repopulation by c-Met-positive stem/progenitor cells isolated from the developing rat liver.	*Hepatogastroenterology*	51	423-6	2004
Numata A, Shimoda K, Kamezaki K, Haro T, Kakumitsu H, Shide K, Kato K, Miyamoto T, Yamashita Y, Oshima Y, Nakajima H, Iwama A, Aoki K, Takase K, Gondo H, Mano H, and Harada M.	Signal transducers and activators of transcription 3 augments the transcriptional activity of CCAAT/enhancer binding protein α in G-CSF signaling pathway.	*J. Biol. Chem.*		In press	2005